EUROPEAN ORGANIZATION FOR NUCLEAR RESEARCH

Centrality and pseudorapidity dependence of the charged-particle multiplicity density in Xe–Xe collisions at $\sqrt{s_{\mathrm{NN}}}$ = 5.44 TeV

ALICE Collaboration[*]

Abstract

In this Letter, the ALICE Collaboration presents the first measurements of the charged-particle multiplicity density, $\mathrm{d}N_{\mathrm{ch}}/\mathrm{d}\eta$, and total charged-particle multiplicity, $N_{\mathrm{ch}}^{\mathrm{tot}}$, in Xe–Xe collisions at a centre-of-mass energy per nucleon–nucleon pair of $\sqrt{s_{\mathrm{NN}}}$ = 5.44 TeV. The measurements are performed as a function of collision centrality over a wide pseudorapidity range of $-3.5 < \eta < 5$. The values of $\mathrm{d}N_{\mathrm{ch}}/\mathrm{d}\eta$ at mid-rapidity and $N_{\mathrm{ch}}^{\mathrm{tot}}$ for central collisions, normalised to the number of nucleons participating in the collision (N_{part}) as a function of $\sqrt{s_{\mathrm{NN}}}$ follow the trends established in previous heavy-ion measurements. The same quantities are also found to increase as a function of N_{part}, and up to the 5% most central collisions the trends are the same as the ones observed in Pb–Pb at a similar energy. For more central collisions, the Xe–Xe scaled multiplicities exceed those in Pb–Pb for a similar N_{part}. The results are compared to phenomenological models and theoretical calculations based on different mechanisms for particle production in nuclear collisions. All considered models describe the data reasonably well within 15%.

[*]See Appendix A for the list of collaboration members

arXiv:1805.04432v2 [nucl-ex] 25 Jan 2019

1 Introduction

A plasma of strongly interacting quarks and gluons is formed in the hot and dense nuclear matter created in ultra-relativistic heavy-ion collisions [1, 2]. The multiplicity of charged particles produced in the collisions is a key observable to characterise the properties of the matter created in these collisions, as the overall particle production is related to the initial energy density. Nuclei are extended objects and the degree of geometrical overlap between them in the collision, expressed in terms of the impact parameter (b), varies. Since b is not directly measurable, an experimental proxy of centrality is used to characterise the amount of nuclear overlap in the collisions. Typical features related to the collision centrality are the number of nucleons participating in the collision, N_{part}, and the number of binary nucleon-nucleon collisions, N_{coll}, among the participant nucleons. Collisions of nuclei of different sizes lead to different N_{part} and N_{coll} for similar relative nuclear overlap. The study of the production of charged particles with different collision systems and at various collision energies can help shed light on the role of the initial energy density and the production mechanism of final-state particles.

Previous measurements of the system-size dependence of the charged-particle pseudorapidity density ($dN_{ch}/d\eta$) were performed at RHIC, comparing Au–Au and Cu–Cu collisions at various centre-of-mass energies [3]. The ALICE, ATLAS and CMS Collaborations at the LHC have previously reported on $dN_{ch}/d\eta$ in Pb–Pb collisions at $\sqrt{s_{NN}} = 2.76$ TeV [4–7] and 5.02 TeV [8, 9]. The dependence of the charged-particle density averaged at mid-rapidity ($|\eta| < 0.5$) $\langle dN_{ch}/d\eta \rangle$ over the centre-of-mass energy shows a steeper increase in central heavy-ion collisions than in proton–proton (pp) and proton–nucleus (pA) collisions. The values of $\langle dN_{ch}/d\eta \rangle$, normalised by the number of nucleon pairs participating in the collision, increase faster than linearly with N_{part}. No significant differences between the shapes of the N_{part} dependence for the different collision energies were observed.

In this Letter, the ALICE Collaboration presents the first measurement of the production of charged, primary particles in Xe–Xe collisions at $\sqrt{s_{NN}} = 5.44$ TeV. The size of the Xe–Xe system is intermediate between previously studied systems at the LHC, Pb–Pb [4, 5, 8, 9] being the largest and p–Pb and pp [10, 11] the smallest. The charged-particle pseudorapidity density is presented over the interval $-3.5 < \eta < 5$ and as a function of the collision centrality. The mid-rapidity values normalised by the number of participating nucleon–nucleon pairs are also reported. The results are also compared with measurements at lower collision energies and with theoretical calculations.

2 Experimental setup

The data were recorded with the ALICE apparatus in 6 hours of stable data-taking with ^{129}Xe beams (16 bunches per beam) colliding at $\sqrt{s_{NN}} = 5.44$ TeV in October 2017. The data were collected with a reduced magnetic field of 0.2 T (as compared to the nominal value of 0.5 T) in the ALICE solenoid magnet. The performance and a detailed description of ALICE can be found elsewhere [12]. In the following, the detector elements relevant to this analysis are briefly described.

The innermost part of the tracking system of ALICE is the Silicon Pixel Detector (SPD) [13] which consists of two cylindrical layers of hybrid silicon pixel assemblies. The inner and outer SPD layers are placed at radii of 3.9 and 7.6 cm from the interaction point and cover $|\eta| < 2$ and $|\eta| < 1.4$, respectively. The Forward Multiplicity Detector (FMD) [14, 15] consists of three sets of silicon strip sensors, covering the pseudorapidities $-3.5 < \eta < -1.8$ and $1.8 < \eta < 5$. The FMD records the energy deposited by charged particles impinging the detector. The V0 detector [15, 16] is used for triggering and centrality classification. It consists of two sub-detectors, V0-A and V0-C, covering the pseudorapidity regions $2.8 < \eta < 5.1$ and $-3.7 < \eta < -1.7$, respectively. The V0 has a timing resolution better than 1 ns, allowing its fast signals to be combined in a programmable logic to reject beam-induced background events while ensuring maximum efficiency for the selection of collision events. The Zero-Degree Calorimeters (ZDCs) [17] are located at a distance of 112.5 m from the interaction point along the beam line, on either

side of the experiment. They measure the energy of spectator (non–interacting) nucleons. The ZDCs are also used for triggering and provide timing information used to select collisions occurring in the interaction point region.

3   Data sample and analysis method

The hadronic interaction rate in ALICE was about 150 (80) Hz at the beginning (end) of the data-taking. The magnetic field of 0.2 T, reduced as compared to normal Pb–Pb settings (0.5 T) increases the acceptance for low-momentum particles, thus enhancing the acceptance of the V0 system for electromagnetic (EM) interactions, which constitute a background for this analysis. In order to suppress this source of contamination, the minimum bias interaction trigger required a signal in each of the V0 sub-detectors in coincidence with a signal in each of the two neutron ZDCs. It was verified by means of a set of control triggers that such a trigger is fully efficient for hadronic interactions in the 0–90% centrality range. In addition, beam-background interactions are removed using the V0 and the ZDC timing information. The interaction probability per bunch-crossing was sufficiently small that the chance of two hadronic interactions occurring within the integration time of the involved detectors, so-called pileup events, was negligible. A total of about 1 million hadronic collisions are used in this analysis.

The classification of collisions into centrality classes uses the sum of the amplitudes of the signals in the V0-A and V0-C detectors. A model of particle production, based on a Glauber description [18, 19], is fitted to the V0 amplitude distribution [20]. The number of particles in the V0 detector is calculated with a two-component model for the number of sources given by

$$N_{\text{sources}} = f \times N_{\text{part}} + (1 - f) \times N_{\text{coll}} \quad , \tag{1}$$

where f constrains the relative contributions of N_{part} and N_{coll}, coupled to a particle production model for each source parameterised by the negative binomial distribution (NBD). In the Glauber calculation, the nuclear density for ^{129}Xe is described by a Woods-Saxon distribution for a deformed nucleus

$$\rho(r, \vartheta) = \rho_0 \frac{1}{1 + \exp\left(\frac{r - R(\vartheta)}{a}\right)} \quad . \tag{2}$$

The parameter ρ_0 is the nucleon density, which provides the overall normalisation. The nuclear skin thickness is $a = 0.59 \pm 0.07$ fm [21]. The nuclear radius R is parametrised as a function of the polar angle ϑ by $R(\vartheta) = R_0[1 + \beta_2 Y_{20}(\vartheta)]$, where R_0 is the average radius and the Legendre polynomial Y_{20} describes the nucleus deformation for an axially symmetric case with no dependence on the azimuthal angle. For the average radius we used $R_0 = 5.4 \pm 0.1$ fm, scaling the results for ^{132}Xe reported in [21] by the atomic mass number (A) dependence of the radius, namely $(129/132)^{1/3}$ [19]. The deformation parameter $\beta_2 = 0.18 \pm 0.02$ is obtained by linearly interpolating the values measured for the Xe A-even isotopes from 124 to 136 [22]. In the Glauber model calculation, the orientation of the spheroid symmetry axis is randomly sampled. For $\sqrt{s_{NN}}$ = 5.44 TeV collisions, an inelastic nucleon–nucleon cross section of 68.4 ± 0.5 mb, obtained by logarithmic interpolation of cross section measurements with respect to collision energies in pp collisions [23], is used. The NBD-Glauber fit provides a good description of the observed V0 amplitude in the region corresponding to the top 90% of the hadronic cross section, where the effects of trigger inefficiency and contamination by EM processes are negligible. The average numbers of participants $\langle N_{\text{part}} \rangle$ reported in Tab. 1 are estimated from the Glauber model imposing the same cuts applied to the data on the simulated V0 response. One should note that the centrality selection based on the V0 amplitude induces a bias on the measured $\langle$dN_{ch}/d$\eta\rangle$. This leads to a $\langle$dN_{ch}/d$\eta\rangle$ in the 70-80% (80-90%) centrality class about 3% (10%) lower than the value one would obtain with a centrality selection based on the impact parameter.

For all the collisions in the 0–90% centrality range the coordinates of the primary interaction point can be reconstructed with good accuracy by correlating hits in the two SPD layers. The measurement of the charged-particle multiplicity density at mid-rapidity uses information from the SPD. The acceptance of the SPD for charged particles spans different pseudorapidity regions depending on the position of the interaction point along the beam line, z. For example, for collisions with the vertex located within $|z| < 7\,\mathrm{cm}$ a maximum acceptance of $|\eta| < 1.5$ can be reached, with approximately constant acceptance for $|\eta| < 0.5$. To extend the pseudorapidity coverage up to $|\eta| < 2$, all collisions with a primary vertex located within $|z| < 20\,\mathrm{cm}$ have been considered.

Following the method developed earlier [4, 5, 8, 9, 24], tracklets (short track segments) are formed using the position of the primary vertex and all possible combinations of hits between the two SPD layers. The primary charged-particle multiplicity density $dN_{ch}/d\eta$ is obtained from the number of tracklets that pass the quality selection criteria, after correcting for detector acceptance, reconstruction and selection efficiencies and contamination from combinatorial background and secondary charged particles. This selection allows primary charged-particle detection down to a momentum of 30 MeV/c. The corrections are estimated using a detailed simulation based on events generated with the HIJING event generator [25] with particle transport in ALICE performed by GEANT3 [26]. The decay products of long-lived decaying particles like K^0_S, Λ, $\bar{\Lambda}$ and other strange hadrons are classified as secondary particles [27] and the contamination from these particles is subtracted from data. It is known that HIJING underestimates the relative production rate of strange particles in high-energy heavy-ion collisions. For this reason, the simulation has been reweighed to reproduce the relative particle abundances observed in the data which are about 30% (50%) higher than HIJING in the most central (peripheral) collisions. The reweighing factors have been derived from an estimate of K^0_S, Λ and $\bar{\Lambda}$ relative production in the data, obtained via invariant mass reconstruction and compared to HIJING.

The deposited energy signal in the FMD is used to measure the charged-particle pseudorapidity density in the forward regions ($-3.5 < \eta < -1.8$ and $1.8 < \eta < 5$), following the method described elsewhere [5]. The energy loss is measured in the 51,200 Si strip sensors of the detector and a statistical approach is used to calculate the inclusive number of charged particles. A data-driven correction derived from previous studies [24] corrects for the background of secondary particles, which are abundant in the forward regions.

4 Systematic uncertainties

The systematic uncertainties on $\langle N_{part} \rangle$ are obtained by varying the parameters of the Glauber model independently within their estimated uncertainties and repeating the NBD-Glauber fit. The uncertainty due to the centrality determination is estimated by changing the value of V0 amplitude that corresponds to the top 90% of the hadronic cross section by ±0.5%. This results in an uncertainty on $\langle dN_{ch}/d\eta \rangle$ of 0.1% to 4.8% from central to peripheral collisions. An additional 4% uncertainty assigned to the most peripheral class, arising from the remaining contamination from EM processes, was estimated by studying the energy deposition in the ZDCs [28].

For the tracklet analysis at mid-rapidity the relative systematic uncertainty on the measurement of the charged-particle multiplicity in peripheral (central) events arises from the following sources: tracklet selection 0.1% (0.8%), calculated by varying the tracklet quality cut up to 4 times the nominal value; combinatorial background subtraction 0.5% (2.0%), estimated from simulations and cross-checked using an alternative method where artificial SPD clusters are added to the data and the number of corresponding artificial reconstructed tracklets are used for background subtraction; particle composition 0.2% (0.2%), estimated by changing the relative abundances of protons, pions and kaons by ±30% in the simulation; contamination by weak decays 0.3% (0.3%), estimated by changing the reweighting factors; extrapolation to zero transverse momentum 0.6% (0.6%), obtained from the variation of the estimated yield of

Centrality	$\langle N_{part} \rangle$	$\langle dN_{ch}/d\eta \rangle$	$\frac{2}{\langle N_{part} \rangle}\langle dN_{ch}/d\eta \rangle$	N_{ch}^{tot}	$\frac{2}{\langle N_{part} \rangle}N_{ch}^{tot}$
0–1%	246 ± 2	1302 ± 17	10.6 ± 0.2	14700 ± 300	119.5 ± 2.6
1–2%	241 ± 2	1223 ± 25	10.1 ± 0.2	13840 ± 250	114.9 ± 2.3
2–3%	236 ± 3	1166 ± 23	9.88 ± 0.23	13250 ± 280	112.3 ± 2.8
3–4%	231 ± 2	1113 ± 20	9.64 ± 0.19	12700 ± 290	110.0 ± 2.7
4–5%	225 ± 3	1069 ± 20	9.50 ± 0.22	12180 ± 260	108.3 ± 2.7
0–2.5%	242 ± 2	1238 ± 25	10.2 ± 0.2	14100 ± 320	116.5 ± 2.8
2.5–5.0%	229 ± 2	1096 ± 27	9.57 ± 0.25	12440 ± 280	108.6 ± 2.6
5.0–7.5%	214 ± 3	986 ± 25	9.21 ± 0.27	11230 ± 330	105.0 ± 3.4
7.5–10%	199 ± 2	891 ± 24	8.95 ± 0.26	10300 ± 300	103.5 ± 3.2
0–5%	236 ± 2	1167 ± 26	9.89 ± 0.24	13230 ± 280	112.1 ± 2.6
5–10%	207 ± 3	939 ± 24	9.07 ± 0.27	10820 ± 280	105.0 ± 3.1
10–20%	165 ± 3	706 ± 17	8.56 ± 0.26	8200 ± 310	99.4 ± 4.2
20–30%	118 ± 4	478 ± 11	8.10 ± 0.33	5670 ± 300	96.1 ± 6.0
30–40%	82.2 ± 3.9	315 ± 8	7.66 ± 0.41	3770 ± 270	91.7 ± 7.9
40–50%	54.6 ± 3.6	198 ± 5	7.25 ± 0.51	2460 ± 220	90.1 ± 10
50–60%	34.1 ± 3.0	118 ± 3	6.92 ± 0.63	1480 ± 170	86.8 ± 13
60–70%	19.7 ± 2.1	64.7 ± 2.0	6.57 ± 0.73	828 ± 44	84.1 ± 10
70–80%	10.5 ± 1.1	32.0 ± 1.3	6.10 ± 0.68	437 ± 16	83.2 ± 9.2
80–90%	5.13 ± 0.46	13.3 ± 0.9	5.19 ± 0.58	181 ± 7.0	70.6 ± 6.9

Table 1: The $\langle dN_{ch}/d\eta \rangle$ and N_{ch}^{tot} values for different centrality classes, defined by V0 multiplicity. The errors are total uncertainties, the statistical contribution being negligible. The values of $\langle N_{part} \rangle$ obtained with the Glauber model are also reported. The errors are obtained by varying the parameters of the NBD-Glauber calculation.

particles at low transverse momentum by a factor of two in the simulation; variations in detector acceptance and efficiency 1% (1%), evaluated by carrying out the analysis for different slices of the z-position of the interaction vertex and with subsamples in azimuth. At forward rapidities, the uncertainties related to the measurement of multiplicity arise from the following sources: the data-driven correction for secondary particles [9] 6.1%; the merging algorithms of signals from Si strips to a single particle 1%; variation in rejection threshold for calculation of the charged-particle multiplicity per event $^{+1\%}_{-2\%}$; particle composition 2%, estimated in the same way as in the tracklet analysis.

The systematic uncertainties from centrality selection and electromagnetic interactions affect the overall normalisation of the results. The total systematic uncertainty, obtained by adding in quadrature all contributions, amounts to 6.4% (2%) for peripheral (central) in $|\eta| < 2$, to 6.9% for $\eta > 3.5$ and to 6.4% elsewhere in the forward region, and is partially correlated over η and between different centrality classes.

5 Results

Figure 1 presents the charged-particle multiplicity density $dN_{ch}/d\eta$ as a function of pseudorapidity for 12 centrality classes. The measurement is obtained from the SPD at mid-rapidity, FMD in forward-rapidities, and combined in regions of overlap ($1.8 < |\eta| < 2$) between the two detectors by taking the weighted average using the non-shared uncertainties as weights. The data are symmetrised around $\eta = 0$, averaging positive and negative η results wherever possible, and extended into the non-measured region $-5 < \eta < -3.5$ by reflecting the $3.5 < \eta < 5$ values around $\eta = 0$. Averaged values (left and right) agree within the uncertainties. Assuming that the charged-particle rapidity density dN_{ch}/dy has Gaussian shape and using an effective Jacobian, the measured $dN_{ch}/d\eta$ is fitted with this ansatz and a width of $\sigma = 4.4 \pm 0.1$ is found, consistent with the value obtained in Pb–Pb at $\sqrt{s_{NN}} = 5.02\,\mathrm{TeV}$ [9].

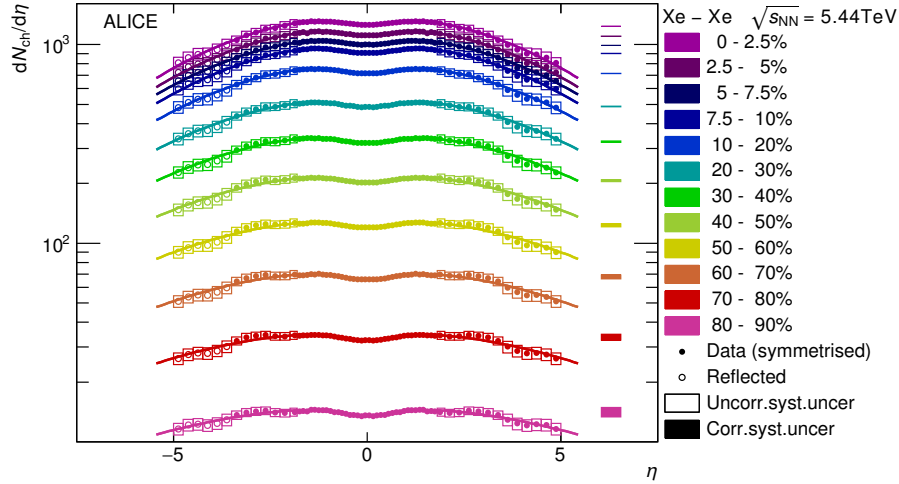The multiplicity density averaged over $|\eta| < 0.5$ in different centrality classes is shown in Tab. 1. The

Fig. 1: Charged–particle pseudorapidity density for 12 centrality classes over a broad η range in Xe–Xe collisions at $\sqrt{s_{NN}} = 5.44\,\text{TeV}$. Boxes around the points reflect the total systematic uncertainties, while the filled squares on the right reflect the normalisation uncertainty from the centrality determination. Statistical errors are negligible. The reflection (open circles) of the $3.5 < \eta < 5$ values around $\eta = 0$ is also shown. The lines correspond to fits to a gaussian distribution in rapidity multiplied by an effective Jacobian of transformation from η to y.

total charged-particle multiplicity N_{ch}^{tot} is determined from the data in the measured region and from extrapolations, up to $\eta = \pm y_{beam}$, in the unmeasured region. Three different functions are used to extrapolate the data points: the difference of two Gaussian distributions centred at $\eta = 0$; a Woods-Saxon-like distribution in rapidity as proposed by PHOBOS [29]; and a trapezoidal form. The trapezoid ansatz in the forward unmeasured regions corresponds to a linear extrapolation up to $\eta = \pm y_{beam}$ with the starting point constrained by the measurements. A Gaussian dN_{ch}/dy in rapidity results in a distribution in pseudorapidity which is very similar to the difference of two Gaussians centered at $\eta = 0$. The central value in the unmeasured regions ($-8.6 < \eta < -3.5$ and $5 < \eta < 8.6$) is taken as the average between the trapezoidal function (which gives the lowest N_{ch}^{tot}) and the Gaussian dN_{ch}/dy (which gives the highest N_{ch}^{tot}). The contribution from the extrapolated region is less than 30% of N_{ch}^{tot}. The systematic uncertainty of the extrapolated N_{ch}^{tot} is calculated as the quadratic sum of contributions from the systematic uncertainty of the data and a conservative contribution obtained by comparing the results from the different fit functions. It amounts to about 14% (4%) of N_{ch}^{tot} in peripheral (central) events. In order to compare bulk particle production at different energies and in different collision systems, the average charged-particle multiplicity density $\langle dN_{ch}/d\eta \rangle$ at mid-rapidity is divided by the average number of participating nucleon pairs, $\langle N_{part} \rangle/2$. This allows one to compare nuclear collisions to pp and p$\bar{\text{p}}$ collisions. The $\langle N_{part} \rangle$ values are calculated within the Glauber model.

Figure 2 (top) shows the mid-rapidity charged-particle multiplicity normalised by the number of nucleon pairs participating in the collision, $\frac{2}{\langle N_{part} \rangle}\langle dN_{ch}/d\eta \rangle$, in pp, p$\bar{\text{p}}$, p(d)A and in central heavy-ion collisions as a function of the centre-of-mass energy. The lines represent fits to lower energy results. The Xe–Xe result is in agreement within the uncertainties with the trend established from previous heavy-ion measurements, which shows a stronger rise as a function of $\sqrt{s_{NN}}$ than for pp and p–Pb collisions. Figure 2 (bottom) shows the total charged-particle multiplicity per participant nucleon pair $\frac{2}{\langle N_{part} \rangle}N_{ch}^{tot}$, which follows the trend for central heavy-ion collisions.

Figure 3 shows the centrality dependence of the mid-rapidity and the total multiplicities per participant nucleon pairs. The point-to-point centrality-dependent uncertainties are indicated by error bars whereas the shaded bands show the correlated uncertainties. The values of $\frac{2}{\langle N_{part} \rangle}\langle dN_{ch}/d\eta \rangle$ and $\frac{2}{\langle N_{part} \rangle}N_{ch}^{tot}$ de-
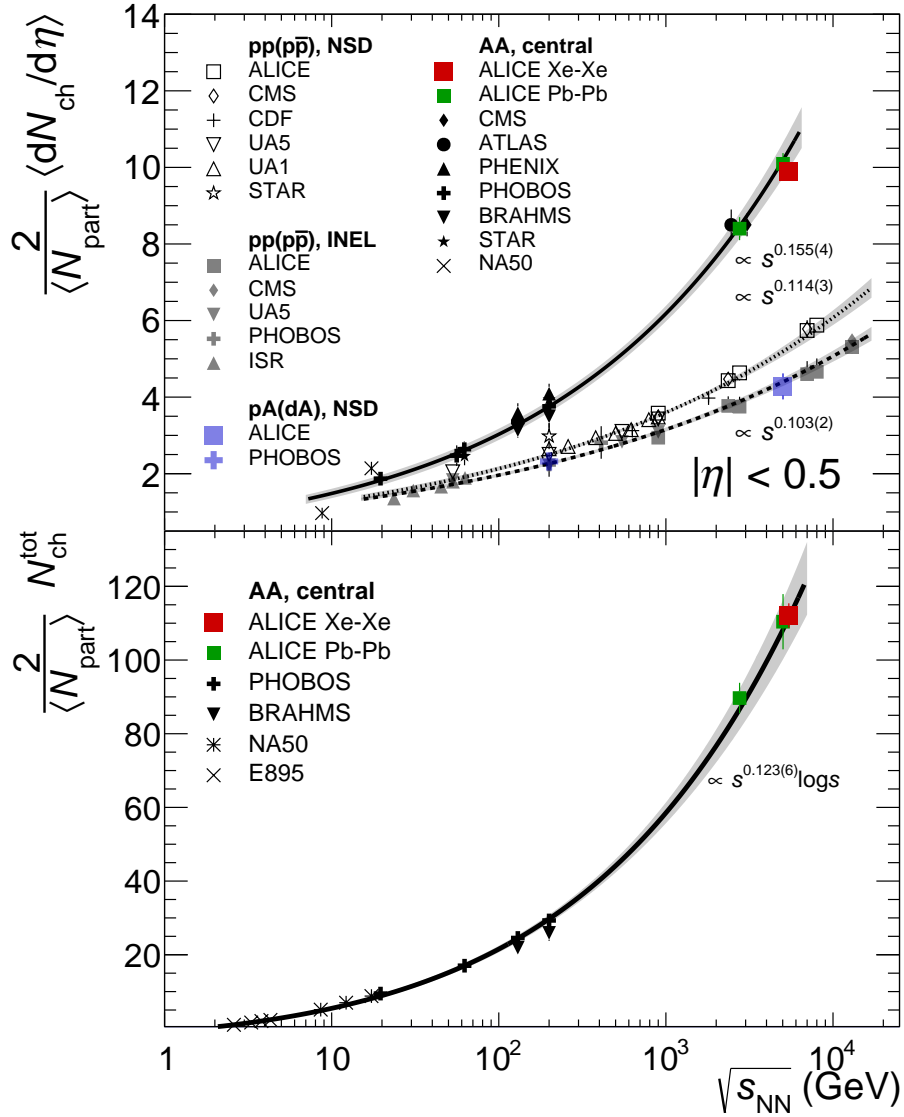
Fig. 2: Values of $\frac{2}{\langle N_{part}\rangle}\langle dN_{ch}/d\eta\rangle$ (top) and $\frac{2}{\langle N_{part}\rangle}N_{ch}^{tot}$ (bottom) for the 5% most central Xe–Xe collisions compared to previous measurements in Pb–Pb [4, 6–9, 30] and Au–Au [3, 31–34] as a function of $\sqrt{s_{NN}}$, as well as for inelastic pp, p$\bar{\text{p}}$ [10, 35, 36] and non-single diffractive pA and dA collisions [11, 37]. The lines are power law fits to the data, excluding Xe–Xe results. The central Pb–Pb measurements from CMS and ATLAS at 2.76 TeV have been shifted horizontally for clarity.

crease by a factor 2 from the most central to the most peripheral collisions, where they agree with the values measured in minimum bias pp and p–Pb collisions [10, 11]. The data are compared to lower energy results at $\sqrt{s_{NN}} = 200\,\text{GeV}$ [3] for the RHIC experiment, $\sqrt{s_{NN}} = 2.76\,\text{TeV}$ [4, 5] and $\sqrt{s_{NN}} = 5.02\,\text{TeV}$ [8, 9] for Pb–Pb collisions where the latter has been re-analysed with the same analysis technique in narrower centrality classes, scaled to match the Xe–Xe data at $\sqrt{s_{NN}} = 5.44\,\text{TeV}$. The scaling factors are calculated using the fit function of Fig. 2 for the top 5% central collisions. For the 5% most central Xe–Xe and for the 2% most central Pb–Pb collisions, the $\frac{2}{\langle N_{part}\rangle}\langle dN_{ch}/d\eta\rangle$ increases steeply. A similar conclusion was also reached for the RHIC data [3]: the Cu–Cu trend resembles that of Au–Au up to the most central collisions and rises above it for the most central collisions. The RHIC data are also shown in Fig. 3 and a deviation from the LHC data for $N_{part} < 100$ is visible, although with large uncertainties. The steeper rise might be due to multiplicity fluctuations in the tail of the Xe–Xe V0 amplitude distribution [22]. The fluctuations occur both in the number of collisions over participants
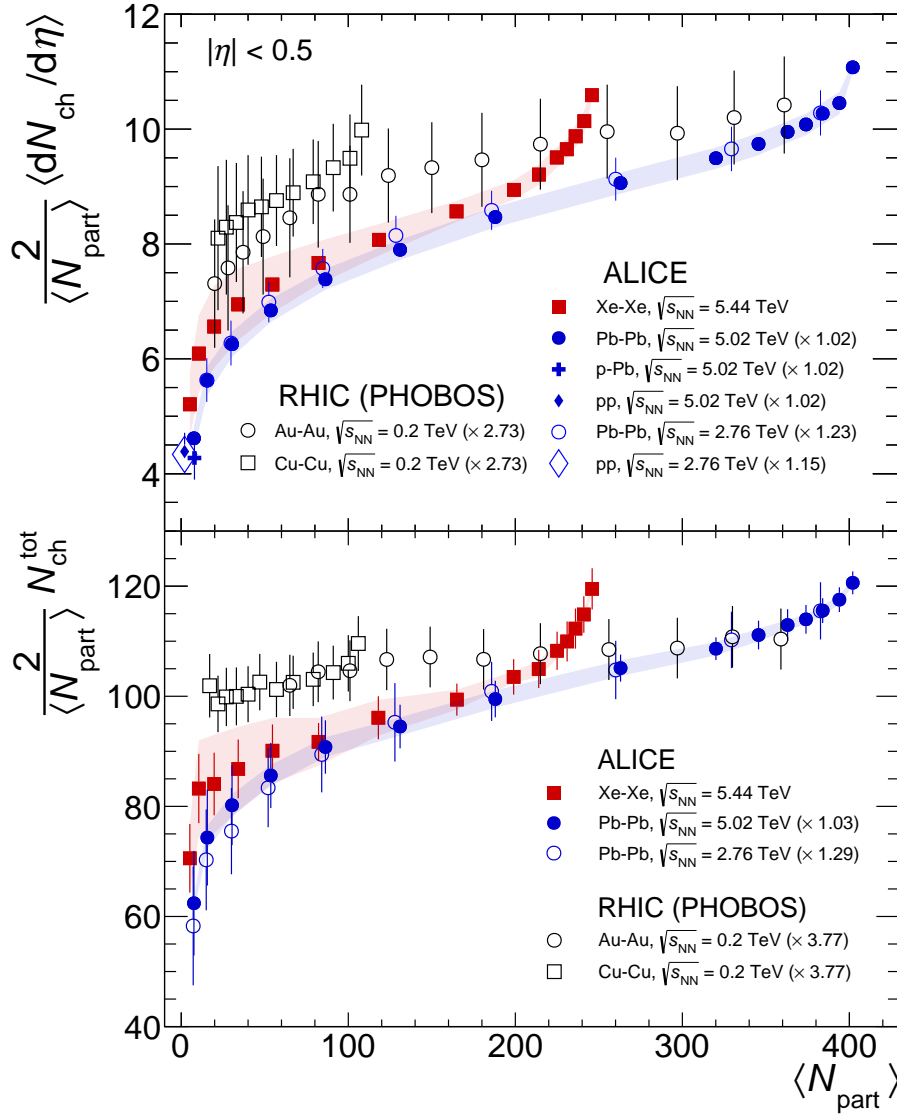
Fig. 3: The $\frac{2}{\langle N_{part}\rangle}\langle dN_{ch}/d\eta\rangle$ (top) and $\frac{2}{\langle N_{part}\rangle}N_{ch}^{tot}$ (bottom) for Xe–Xe collisions at $\sqrt{s_{NN}} = 5.44$ TeV as a function of $\langle N_{part}\rangle$. The error bars indicate the point-to-point centrality-dependent uncertainties whereas the shaded band shows the correlated contributions. Also shown in the figure is the result from inelastic pp at $\sqrt{s} = 5.02$ TeV as well as non-single diffractive p–Pb collisions [11] and Pb–Pb collisions at $\sqrt{s_{NN}} = 5.02$ TeV [8, 9]. Note that Pb–Pb data at $\sqrt{s_{NN}} = 5.02$ TeV were re-analysed in narrower centrality classes. Data from lower energies at $\sqrt{s_{NN}} = 2.76$ TeV [4, 5] and 200 GeV [3] are shown for comparison.

and in the number of charged particles over participants. The rise is quantitatively reproduced by the NBD-Glauber fit. The total number of charged particles scaled by the number of participant pairs shows a slight increase as a function of the number of participants in Fig. 3 (bottom), similar to that of the midrapidity results, albeit with larger experimental uncertainties. Figure 4 shows the Xe–Xe and Pb–Pb results as a function of a different scaling variable $(\langle N_{part}\rangle - 2)/(2A)$, where A is the atomic mass number of the colliding nucleus. The figure shows that $\frac{2}{\langle N_{part}\rangle}\langle dN_{ch}/d\eta\rangle$ and $\frac{2}{\langle N_{part}\rangle}N_{ch}^{tot}$ have a similar dependence on the number of participants relative to the possible maximum number of participants, which indicates a stronger dependence on geometric properties of the collision zone than on the collision system sizes.

The study of the centrality dependence of particle multiplicity for different collision systems provides a variable number of nucleon-nucleon collisions at equal number of participating nucleons and there-
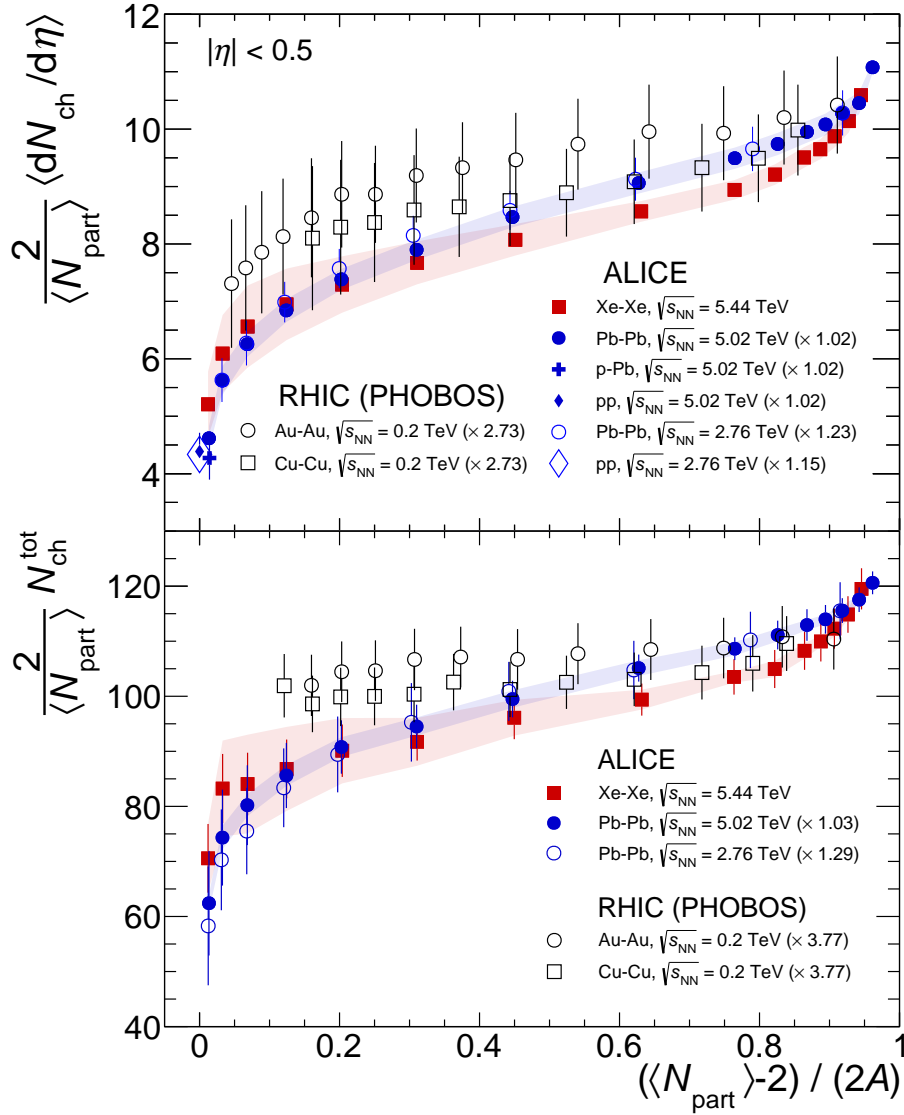
Fig. 4: The $\frac{2}{\langle N_{\mathrm{part}} \rangle} \langle \mathrm{d}N_{\mathrm{ch}}/\mathrm{d}\eta \rangle$ (top) and $\frac{2}{\langle N_{\mathrm{part}} \rangle} N_{\mathrm{ch}}^{\mathrm{tot}}$ (bottom) for Xe–Xe collisions at $\sqrt{s_{\mathrm{NN}}} = 5.44\,\mathrm{TeV}$ as a function of $(\langle N_{\mathrm{part}} \rangle - 2)/(2A)$.

fore may provide further information to clarify the measured deviation from N_{part} scaling. The scaling of the charged-particle multiplicity by the number of participant nucleons was studied in detail and a deviation from N_{part}-scaling was observed at RHIC energies [3, 30, 38–40]. The deviation from N_{part}-scaling was initially thought to be due to a relative increase in hard processes in central collisions, but no conclusive evidence was found to support this interpretation. Figure 5 compares $\frac{2}{\langle N_{\mathrm{part}} \rangle} \langle \mathrm{d}N_{\mathrm{ch}}/\mathrm{d}\eta \rangle$ in Xe–Xe collisions at $\sqrt{s_{\mathrm{NN}}} = 5.44\,\mathrm{TeV}$ with different parameterisations for particle production. Specifically, we used the two-component model in Eq. 1 and two power-law functions $\langle \mathrm{d}N_{\mathrm{ch}}/\mathrm{d}\eta \rangle \propto N_{\mathrm{part}}^{\alpha}$ and $\langle \mathrm{d}N_{\mathrm{ch}}/\mathrm{d}\eta \rangle \propto N_{\mathrm{coll}}^{\beta}$. The functions were fitted to the Pb–Pb data at $\sqrt{s_{\mathrm{NN}}} = 5.02\,\mathrm{TeV}$ [8]. For the Xe–Xe data only the absolute normalisation was adjusted. The values of the parameters are also consistent with those obtained at SPS and RHIC energies [30, 41]. While no unique physics conclusion can be drawn from such fits, this suggests that geometrical arguments may be sufficient to provide a good description of particle production across different colliding systems and beam energies.

Describing particle production in relativistic heavy-ion collisions as a superposition of emission from a thermal core and hard scatterings in a corona [42], one can classify the participating nucleons into those
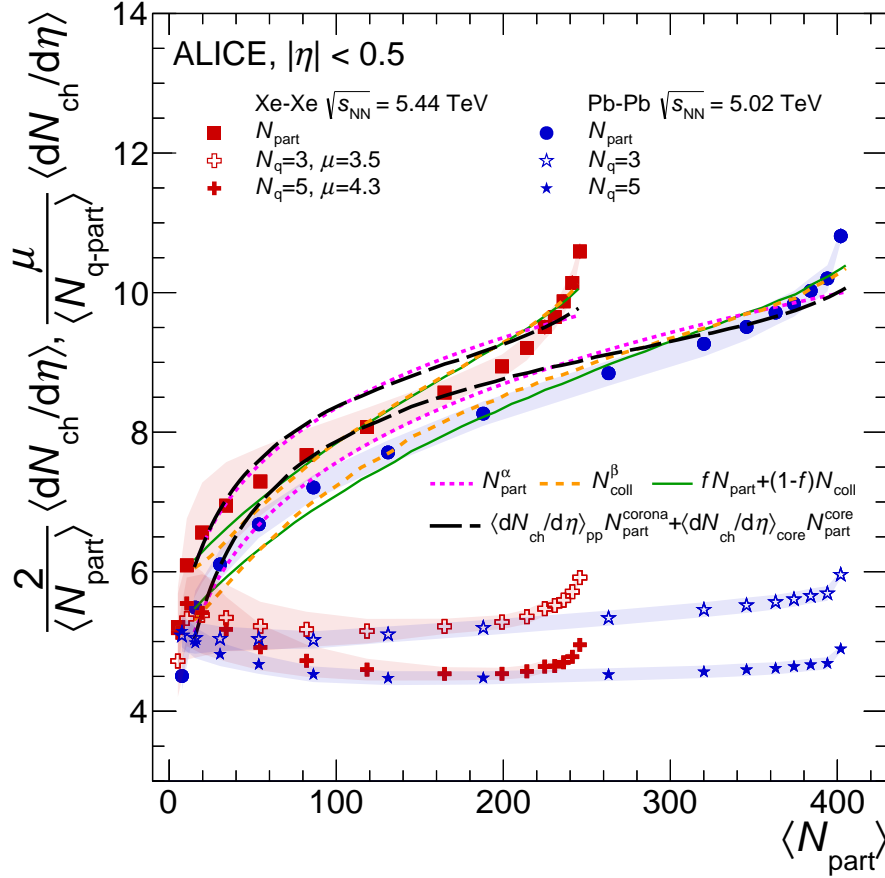
Fig. 5: The $\frac{2}{\langle N_{part}\rangle}\langle dN_{ch}/d\eta\rangle$ for Xe–Xe collisions at $\sqrt{s_{NN}}$ = 5.44 TeV and Pb–Pb collisions at $\sqrt{s_{NN}}$ = 5.02 TeV [8], as a function of $\langle N_{part}\rangle$. The Pb–Pb data are fitted with various parameterisations of N_{part} and N_{coll}, calculated with the Glauber model. The same functions, with the values of the parameters from the Pb–Pb fit, are used for the Xe–Xe data. Also shown is $\langle dN_{ch}/d\eta\rangle$ per participant quark, $N_{q\text{-part}}$, calculated with the effective wounded constituent quarks model [43], as a function of $\langle N_{part}\rangle$. The number of participant quarks $N_{q\text{-part}}$ is normalised by the average number of participant quarks in pp collisions, μ.

that scatter only once (N_{part}^{corona}) and those that scatter multiple times (N_{part}^{core}). The multiplicity can then be fitted with the sum of those contributions, $\langle dN_{ch}/d\eta\rangle_{pp} N_{part}^{corona} + \langle dN_{ch}/d\eta\rangle_{core} N_{part}^{core}$, where $\langle dN_{ch}/d\eta\rangle_{pp}$ is the multiplicity measured in inelastic pp collisions [10] and $\langle dN_{ch}/d\eta\rangle_{core}$ is the contribution to the charged-particle multiplicity from the core of the fireball, which is fitted to the data. Figure 5 also shows $\langle dN_{ch}/d\eta\rangle$ per participant quark $N_{q\text{-part}}$ calculated with a Glauber model using effective wounded constituent quarks [44][43], as a function of N_{part}, as was done for Pb–Pb collisions at $\sqrt{s_{NN}}$ = 5.02 TeV [45] that have been re-analysed in narrower centrality classes. In the implementation of the quark-Glauber model the partonic degrees of freedom (3 or 5) are located around the nucleon centres [43]. The effective inelastic scattering cross section for collisions of constituent quarks is set to 20.38 mb and 9.76 mb, for $N_q = 3$ and $N_q = 5$, respectively, adjusted to reproduce the 68.4 mb nucleon–nucleon inelastic cross section at 5.44 TeV. $N_{q\text{-part}}$ has been divided by the average value in pp collisions $\mu = \langle N_{q\text{-part}}\rangle$, which is 3.5 (4.3) for $N_q = 3$ ($N_q = 5$). Comparing the behaviour of $\langle dN_{ch}/d\eta\rangle$ in terms of the dependence on the number of nucleon or quark participants in the collision, one concludes that $N_{q\text{-part}}$ scaling describes the data better than N_{part} scaling as previously observed [40, 45] except the 0–10% centrality range in Xe–Xe collisions where a clear scaling violation is observed.

Figure 6 shows a comparison of the Xe–Xe data to calculations from theoretical models at mid-rapidity. HIJING 2.1 [46, 47] combines perturbative QCD processes with soft interactions, and includes a strong
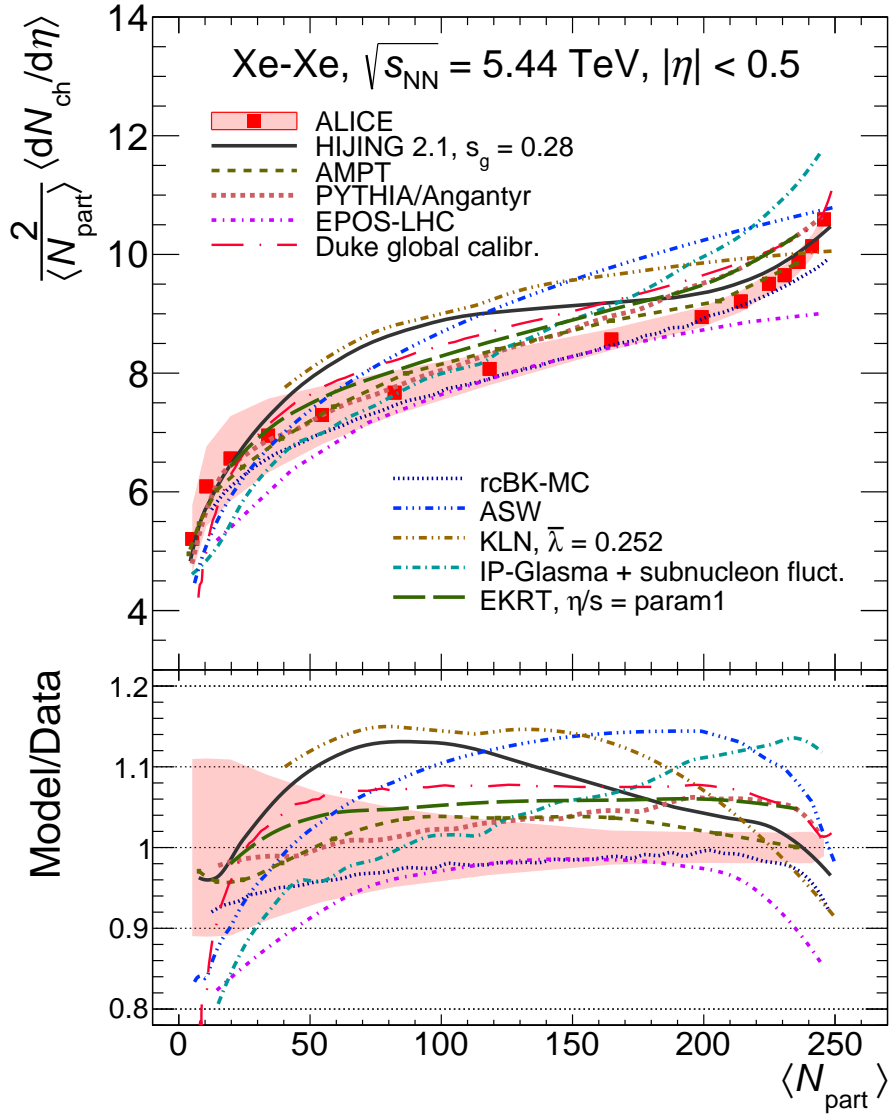
Fig. 6: The $\frac{2}{\langle N_{part} \rangle} \langle dN_{ch}/d\eta \rangle$ for Xe–Xe collisions at $\sqrt{s_{NN}} = 5.44$ TeV as a function of $\langle N_{part} \rangle$ compared to model predictions [46, 47, 49–65]. The bottom panel shows the ratio of the models to the data. The shaded band around the points reflects the correlated systematic uncertainties.

impact parameter dependence of parton shadowing [48]. For Xe–Xe data at $\sqrt{s_{NN}} = 5.44$ TeV it uses a large gluon shadowing parameter of 0.28 to limit the multiplicity per participant. With this choice, the same as in Pb–Pb collisions at $\sqrt{s_{NN}} = 5.02$ TeV, the multiplicities at mid-rapidity and the centrality dependence in the most central collisions are reproduced. AMPT [50, 51] is a model which implements hydrodynamical evolution of an initial state produced by HIJING. It includes spatial coalescence of quarks to hadrons, followed by hadronic scattering. AMPT describes both the shape and the overall magnitude of the mid-rapidity data. PYTHIA/Angantyr [52] extends the nucleon–nucleon model of PYTHIA 8.230 [53] to the case of heavy-ion collisions, essentially performing individual nucleon–nucleon collisions at the parton level, while the resulting Lund-strings are hadronised as an ensemble. It is interesting to note that this model agrees reasonably well with the data even though it was developed as an extension of a generator for nucleon–nucleon collisions. EPOS LHC [49] is a parton model based on the Gribov-Regge theory, designed for minimum bias hadronic interactions, which incorporates collective effects treated via a flow parameterisation and a separation of the initial state into core–corona parts. The shape of the centrality dependence is reproduced fairly well at intermediate centralities, however,
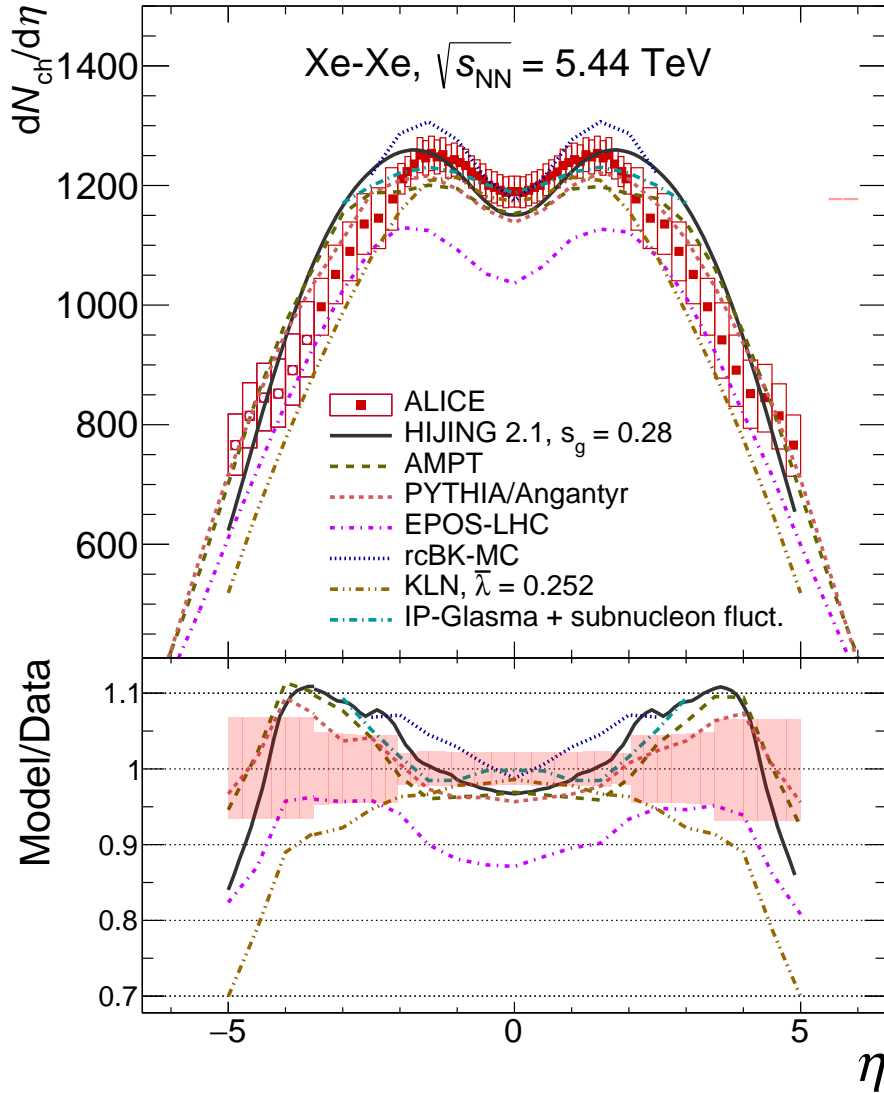
Fig. 7: Comparison of $\mathrm{d}N_{\mathrm{ch}}/\mathrm{d}\eta$ as a function of η in the 0–5% central class to model predictions. The bottom panel shows the ratio of the models to the data. Boxes around the points reflect the total uncorrelated systematic uncertainties.

the model underestimates the absolute values of the multiplicity, as was the case in Pb–Pb collisions at $\sqrt{s_{\mathrm{NN}}} = 5.02\,\mathrm{TeV}$ [8]. The Duke global calibrated model is based on a Bayesian Statistics analysis using $\mathrm{T_R ENTo}$ initial conditions for high-energy nuclear collisions [66, 67]. The subsequent transport dynamics is then simulated using the iEBE-VISHNU event-by-event simulations for relativistic heavy-ion collisions which uses a hybrid approach based on (2 + 1)-dimensional viscous hydrodynamics coupled to a hadronic cascade model [68]. The Duke global calibrated model can reproduce the shape of the mid-rapidity distribution, but overestimates slightly the overall magnitude.

Saturation-inspired models (rcBK-MC [54, 55], KLN [56–59], ASW [60], IP-Glasma [61, 62] and EKRT [63–65]) rely on perturbative QCD and an energy-dependent saturation scale, which limits the number of produced partons, and in turn the number of produced particles. This results in a factorisation of the energy and centrality dependence of particle production or, in other words, in the invariance of the centrality growth, as observed in the experimental data [69]. The rcBK-MC model limits the centrality growth using the rc-BK equation. It provides a good description of the mid-rapidity data, both of the shape and the highest multiplicity reached in central collisions. The ASW prediction overestimates the

data, while it was very accurate in Pb–Pb at $\sqrt{s_{NN}} = 5.02$ TeV. The KLN model does not describe the shape well and, although it agrees with the value measured for most central collisions, it is significantly above the centrality dependence of the data. The IP-Glasma model naturally produces initial energy fluctuations computed within the Color Glass Condensate framework combining an impact parameter dependent saturation model. It uses a gluon multiplicity scaled to describe hadron multiplicities measured in Pb–Pb collisions at $\sqrt{s_{NN}} = 5.02$ TeV [8]. The centrality dependence is stronger than that observed in mid-rapidity data over(under)-predicting the data in central (peripheral) collisions. The EKRT model for heavy-ion collisions uses perturbative QCD with a conjecture of gluon saturation to suppress soft parton production. The saturation scale is also dependent on the local product of thickness functions, implying a geometrical scaling. The space-time evolution of the system is then described with viscous fluid dynamics event-by-event. The normalisation is fixed by exploiting the 0–5% most central multiplicity measurement in Pb–Pb collisions at $\sqrt{s_{NN}} = 2.76$ TeV [70]. As for Pb–Pb collisions at $\sqrt{s_{NN}} = 5.02$ TeV, the EKRT model can describe both the shape and the overall magnitude of multiplicity on centrality. In general, almost all models reproduce the steep rise versus $\langle N_{part} \rangle$ while EPOS-LHC, ASW and KLN show a saturation behaviour. The predictions show a similar trend as for the Pb–Pb case [8] and altogether a flatter distribution with respect to data.

In Fig. 7, the models are compared to the pseudorapidity dependence of the $dN_{ch}/d\eta$ for the top 5% central collisions. HIJING 2.1 reproduces the pseudorapidity dependence at mid-rapidity well, but overestimates the data at forward rapidity, due to the large value of the shadowing parameter used. AMPT and PYTHIA/Angantyr describe the data fairly well, with a slight overestimate at forward rapidities. EPOS LHC reproduces the shape well, but under-predicts the multiplicity overall. The rcBK-MC is restricted to $|\eta| < 2.5$ since its formalism can only be used for rapidities far from the fragmentation regions. It shows a narrower distribution than what is seen in data. KLN agrees with the data at mid-rapidity, but not at forward rapidity, where it under-predicts the data. For IP-Glasma the rapidity dependence is provided by the IP-Sat model [71] and it is converted to pseudorapidity using an effective mass of 0.2 GeV/c^2. The shape is wider than that of the data. Regarding the case of the pseudorapidity dependence all the models show similar trends as for Pb–Pb collisions [9] except HIJING 2.1 which describes the Xe–Xe measurements better than the Pb–Pb data.

6 Conclusions

The measurements of the charged-particle multiplicity density and its centrality dependence in Xe–Xe collisions at $\sqrt{s_{NN}} = 5.44$ TeV have been presented over the pseudorapidity range $-3.5 < \eta < 5$ using the full acceptance of the ALICE detector. For the 5% most central collisions, the average charged-particle pseudorapidity density at mid-rapidity ($|\eta| < 0.5$) is 1167 ± 26 and the total number of charged particles is 13230 ± 280. Scaled by the number of participant pairs, these are found to follow the same power-law dependence with energy established in previous heavy-ion measurements.

The centrality dependences of $\frac{2}{\langle N_{part} \rangle} \langle dN_{ch}/d\eta \rangle$ and $\frac{2}{\langle N_{part} \rangle} N_{ch}^{tot}$ are very similar to those previously measured in Pb–Pb collisions at similar or lower energies up to the 5% most central Xe–Xe collisions, where the Xe–Xe results are larger than the Pb–Pb results at a similar number of participating nucleons. Similar conclusions were drawn at RHIC from the comparison of the data for Cu–Cu and Au–Au collisions [72]. The steeper rise might be due to multiplicity fluctuations in the tail of the Xe–Xe V0 amplitude.

While measurements of particle production in large and medium-sized colliding systems such as Xe–Xe are abundant and become even more precise, the underlying mechanism to describe the increase with energy and centrality is still not completely understood. Deeper insight of the system size dependence of particle production may come from the study of light-nuclei collisions, still not much explored at high energy, which could bridge the gap between the trends observed in pp and pA collisions and those of the mid-sized Xe–Xe and the large Pb–Pb systems.

Acknowledgements

References

[1] F. Karsch, "Lattice QCD at high temperature and density," *Lect. Notes Phys.* **583** (2002) 209–249, `arXiv:hep-lat/0106019 [hep-lat]`.

[2] B. Muller, J. Schukraft, and B. Wyslouch, "First results from Pb+Pb collisions at the LHC," *Ann. Rev. Nucl. Part. Sci.* **62** (2012) 361–386, `arXiv:1202.3233 [hep-ex]`.

[3] **PHOBOS** Collaboration, B. Alver *et al.*, "PHOBOS results on charged particle multiplicity and pseudorapidity distributions in Au+Au, Cu+Cu, d+Au, and p+p collisions at ultra-relativistic energies," *Phys. Rev.* **C83** (2011) 024913, `arXiv:1011.1940 [nucl-ex]`.

[4] **ALICE** Collaboration, K. Aamodt *et al.*, "Centrality dependence of the charged-particle multiplicity density at mid-rapidity in Pb-Pb collisions at $\sqrt{s_{NN}}$ = 2.76 TeV," *Phys. Rev. Lett.* **106** (2011) 032301, `arXiv:1012.1657 [nucl-ex]`.

[5] **ALICE** Collaboration, E. Abbas *et al.*, "Centrality dependence of the pseudorapidity density distribution for charged particles in Pb–Pb collisions at $\sqrt{s_{NN}}$ = 2.76 TeV," *Phys. Lett.* **B726** (2013) 610–622, `arXiv:1304.0347 [nucl-ex]`.

[6] **ATLAS** Collaboration, G. Aad *et al.*, "Measurement of the centrality dependence of the charged particle pseudorapidity distribution in lead-lead collisions at $\sqrt{s_{NN}}$ = 2.76 TeV with the ATLAS detector," *Phys. Lett.* **B710** (2012) 363–382, `arXiv:1108.6027 [hep-ex]`.

[7] **CMS** Collaboration, S. Chatrchyan *et al.*, "Dependence on pseudorapidity and on centrality of charged hadron production in PbPb collisions at $\sqrt{s_{NN}}$ = 2.76 TeV," *JHEP* **08** (2011) 141, `arXiv:1107.4800 [nucl-ex]`.

[8] **ALICE** Collaboration, J. Adam *et al.*, "Centrality dependence of the charged-particle multiplicity density at midrapidity in Pb-Pb collisions at $\sqrt{s_{NN}}$ = 5.02 TeV," *Phys. Rev. Lett.* **116** (2016) 222302, `arXiv:1512.06104 [nucl-ex]`.

[9] **ALICE** Collaboration, J. Adam *et al.*, "Centrality dependence of the pseudorapidity density distribution for charged particles in Pb-Pb collisions at $\sqrt{s_{NN}}$ = 5.02 TeV," *Phys. Lett.* **B772** (2017) 567–577, `arXiv:1612.08966 [nucl-ex]`.

[10] **ALICE** Collaboration, J. Adam *et al.*, "Charged-particle multiplicities in proton–proton collisions at $\sqrt{s}$ = 0.9 to 8 TeV," *Eur. Phys. J.* **C77** no. 1, (2017) 33, `arXiv:1509.07541 [nucl-ex]`.

[11] **ALICE** Collaboration, B. Abelev *et al.*, "Pseudorapidity density of charged particles in p + Pb collisions at $\sqrt{s_{NN}}$ = 5.02 tev," *Phys. Rev. Lett.* **110** (2013) 032301. `http://link.aps.org/doi/10.1103/PhysRevLett.110.032301`.

[12] **ALICE** Collaboration, B. Abelev *et al.*, "Performance of the ALICE Experiment at the CERN LHC," *Int. J. Mod. Phys.* **A29** (2014) 1430044, `arXiv:1402.4476 [nucl-ex]`.

[13] R. Santoro *et al.*, "The ALICE Silicon Pixel Detector: Readiness for the first proton beam," *JINST* **4** (2009) P03023.

[14] C. H. Christensen, J. J. Gaardhoje, K. Gulbrandsen, B. S. Nielsen, and C. Sogaard, "The ALICE Forward Multiplicity Detector," *Int. J. Mod. Phys.* **E16** (2007) 2432–2437, `arXiv:0712.1117 [nucl-ex]`.

[15] **ALICE** Collaboration, P. Cortese *et al.*, *ALICE forward detectors: FMD, TO and VO: Technical Design Report*. Technical Design Report ALICE. CERN, Geneva, 2004. `https://cds.cern.ch/record/781854`. Submitted on 10 Sep 2004.

[16] **ALICE** Collaboration, E. Abbas *et al.*, "Performance of the ALICE VZERO system," *JINST* **8** (2013) P10016, `arXiv:1306.3130 [nucl-ex]`.

[17] E. Puddu *et al.*, "The zero degree calorimeters for the ALICE experiment," *Nuclear Instruments and Methods in Physics Research Section A: Accelerators, Spectrometers, Detectors and Associated Equipment* **581** no. 1, (2007) 397 – 401. VCI 2007.

[18] B. Alver, M. Baker, C. Loizides, and P. Steinberg, "The PHOBOS Glauber Monte Carlo," `arXiv:0805.4411 [nucl-ex]`.

[19] C. Loizides, J. Nagle, and P. Steinberg, "Improved version of the PHOBOS Glauber Monte Carlo," *SoftwareX* **1-2** (2015) 13–18, `arXiv:1408.2549 [nucl-ex]`.

[20] **ALICE** Collaboration, B. Abelev *et al.*, "Centrality determination of Pb-Pb collisions at $\sqrt{s_{NN}} = 2.76\,\text{TeV}$ with ALICE," *Phys. Rev.* **C88** no. 4, (2013) 044909, `arXiv:1301.4361 [nucl-ex]`.

[21] K. Tsukada *et al.*, "First elastic electron scattering from ^{132}Xe at the SCRIT facility," *Phys. Rev. Lett.* **118** no. 26, (2017) 262501, `arXiv:1703.04278 [nucl-ex]`.

[22] **ALICE Collaboration** Collaboration, "Centrality determination using the Glauber model in Xe-Xe collisions at $\sqrt{s_{NN}} = 5.44\,\text{TeV}$," . `http://cds.cern.ch/record/2315401`.

[23] C. Loizides, J. Kamin, and D. d'Enterria, "Precision Monte Carlo Glauber predictions at present and future nuclear colliders," `arXiv:1710.07098 [nucl-ex]`.

[24] **ALICE** Collaboration, J. Adam *et al.*, "Centrality evolution of the charged-particle pseudorapidity density over a broad pseudorapidity range in Pb-Pb collisions at $\sqrt{s_{NN}} = 2.76\,\text{TeV}$," *Phys. Lett.* **B754** (2016) 373–385, `arXiv:1509.07299 [nucl-ex]`.

[25] X.-N. Wang and M. Gyulassy, "HIJING: A Monte Carlo model for multiple jet production in pp, p–A and A–A collisions," *Phys. Rev.* **D44** (1991) 3501–3516.

[26] R. Brun, F. Bruyant, F. Carminati, S. Giani, M. Maire, A. McPherson, G. Patrick, and L. Urban, "GEANT Detector Description and Simulation Tool," . `https://cds.cern.ch/record/1082634`.

[27] **ALICE** Collaboration, "The ALICE definition of primary particles," . `https://cds.cern.ch/record/2270008`.

[28] **ALICE** Collaboration, B. Abelev *et al.*, "Measurement of the Cross Section for Electromagnetic Dissociation with Neutron Emission in Pb-Pb Collisions at $\sqrt{s_{NN}} = 2.76\,\text{TeV}$," *Phys. Rev. Lett.* **109** (2012) 252302, `arXiv:1203.2436 [nucl-ex]`.

[29] **PHOBOS** Collaboration, B. Alver *et al.*, "Charged-particle multiplicity and pseudorapidity distributions measured with the PHOBOS detector in Au+Au, Cu+Cu, d+Au, p+p collisions at ultrarelativistic energies," *Phys. Rev.* **C83** (2011) 024913, `arXiv:1011.1940 [nucl-ex]`.

[30] **NA50** Collaboration, M. C. Abreu *et al.*, "Scaling of charged particle multiplicity in Pb-Pb collisions at SPS energies," *Phys. Lett.* **B530** (2002) 43–55.

[31] **BRAHMS** Collaboration, I. G. Bearden *et al.*, "Charged particle densities from Au+Au collisions at $\sqrt{s_{NN}} = 130$ GeV," *Phys. Lett.* **B523** (2001) 227–233, arXiv:nucl-ex/0108016 [nucl-ex].

[32] **BRAHMS** Collaboration, I. G. Bearden *et al.*, "Pseudorapidity distributions of charged particles from Au+Au collisions at the maximum RHIC energy," *Phys. Rev. Lett.* **88** (2002) 202301, arXiv:nucl-ex/0112001 [nucl-ex].

[33] **PHENIX** Collaboration, K. Adcox *et al.*, "Centrality dependence of charged particle multiplicity in Au-Au collisions at $\sqrt{s_{NN}} = 130$ GeV," *Phys. Rev. Lett.* **86** (2001) 3500–3505, arXiv:nucl-ex/0012008 [nucl-ex].

[34] **STAR** Collaboration, B. I. Abelev *et al.*, "Systematic measurements of identified particle spectra in pp, d + Au and Au + Au collisions from STAR," *Phys. Rev.* **C79** (2009) 034909, arXiv:0808.2041 [nucl-ex].

[35] **CMS** Collaboration, V. Khachatryan *et al.*, "Pseudorapidity distribution of charged hadrons in proton-proton collisions at $\sqrt{s} = 13$ TeV," *Phys. Lett.* **B751** (2015) 143–163, arXiv:1507.05915 [hep-ex].

[36] **ALICE** Collaboration, J. Adam *et al.*, "Pseudorapidity and transverse-momentum distributions of charged particles in protonproton collisions at $\sqrt{s} = 13$ TeV," *Phys. Lett.* **B753** (2016) 319–329, arXiv:1509.08734 [nucl-ex].

[37] **PHOBOS** Collaboration, B. B. Back *et al.*, "Pseudorapidity distribution of charged particles in d + Au collisions at $\sqrt{s_{NN}} = 200$ GeV," *Phys. Rev. Lett.* **93** (2004) 082301, arXiv:nucl-ex/0311009 [nucl-ex].

[38] **NA57 and WA97s** Collaboration, F. Antinori *et al.*, "Determination of the event centrality in the WA97 and NA57 experiments," *J.Phys.* **G27** (2001) 391–396.

[39] **WA98** Collaboration, M. M. Aggarwal *et al.*, "Scaling of Particle and Transverse Energy Production in ^{208}Pb+^{208}Pb collisions at 158 A GeV," *Eur. Phys. J.* **C18** (2001) 651–663.

[40] **PHENIX** Collaboration, A. Adare *et al.*, "Transverse energy production and charged-particle multiplicity at midrapidity in various systems from $\sqrt{s_{NN}} = 7.7$ to 200 GeV," *Phys. Rev.* **C93** no. 2, (2016) 024901, arXiv:1509.06727 [nucl-ex].

[41] **PHENIX** Collaboration, S. S. Adler *et al.*, "Systematic studies of the centrality and $\sqrt{s_{NN}}$ dependence of the $dE(T)/d\eta$ and d $dN_{ch}/d\eta$ in heavy ion collisions at mid-rapidity," *Phys. Rev.* **C71** (2005) 034908, arXiv:nucl-ex/0409015 [nucl-ex]. [Erratum: Phys. Rev.C71,049901(2005)].

[42] K. Werner, "Core-corona separation in ultra-relativistic heavy ion collisions," *Phys. Rev. Lett.* **98** (2007) 152301, arXiv:0704.1270 [nucl-th].

[43] C. Loizides, "Glauber modeling of high-energy nuclear collisions at the subnucleon level," *Phys. Rev.* **C94** no. 2, (2016) 024914, arXiv:1603.07375 [nucl-ex].

[44] S. Eremin and S. Voloshin, "Nucleon participants or quark participants?," *Phys. Rev.* **C67** (2003) 064905, arXiv:nucl-th/0302071 [nucl-th].

[45] **ALICE** Collaboration, J. Adam *et al.*, "Centrality dependence of the charged-particle multiplicity density at midrapidity in Pb-Pb collisions at $\sqrt{s_{NN}}$ = 5.02 TeV,". https://cds.cern.ch/record/2118084.

[46] R. Xu, W.-T. Deng, and X.-N. Wang, "Nuclear modification of high-pT hadron spectra in p+A collisions at LHC," *Phys. Rev.* **C86** (2012) 051901, arXiv:1204.1998 [nucl-th].

[47] W.-T. Deng, X.-N. Wang, and R. Xu, "Hadron production in p+p, p+Pb, and Pb+Pb collisions with the HIJING 2.0 model at energies available at the CERN Large Hadron Collider," *Phys. Rev.* **C83** (2011) 014915, arXiv:1008.1841 [hep-ph].

[48] **European Muon** Collaboration, J. Ashman *et al.*, "Measurement of the ratios of deep inelastic muon - nucleus cross-sections on various nuclei compared to deuterium," *Phys. Lett.* **B202** (1988) 603–610.

[49] T. Pierog, I. Karpenko, J. M. Katzy, E. Yatsenko, and K. Werner, "EPOS LHC: Test of collective hadronization with data measured at the CERN Large Hadron Collider," *Phys. Rev.* **C92** no. 3, (2015) 034906, arXiv:1306.0121 [hep-ph].

[50] Z.-W. Lin, C. M. Ko, B.-A. Li, B. Zhang, and S. Pal, "A Multi-phase transport model for relativistic heavy ion collisions," *Phys. Rev.* **C72** (2005) 064901, arXiv:nucl-th/0411110 [nucl-th].

[51] J. Xu and C. M. Ko, "Pb-Pb collisions at $\sqrt{s_{NN}}$ = 2.76 TeV in a multiphase transport model," *Phys. Rev.* **C83** (2011) 034904, arXiv:1101.2231 [nucl-th].

[52] C. Bierlich, G. Gustafson, and L. Lönnblad, "Diffractive and non-diffractive wounded nucleons and final states in pA collisions," *JHEP* **10** (2016) 139, arXiv:1607.04434 [hep-ph].

[53] T. Sjöstrand, S. Ask, J. R. Christiansen, R. Corke, N. Desai, P. Ilten, S. Mrenna, S. Prestel, C. O. Rasmussen, and P. Z. Skands, "An Introduction to PYTHIA 8.2," *Comput. Phys. Commun.* **191** (2015) 159–177, arXiv:1410.3012 [hep-ph].

[54] J. L. Albacete, A. Dumitru, H. Fujii, and Y. Nara, "CGC predictions for p + Pb collisions at the LHC," *Nucl. Phys.* **A897** (2013) 1–27, arXiv:1209.2001 [hep-ph].

[55] J. L. Albacete and A. Dumitru, "A model for gluon production in heavy-ion collisions at the LHC with rcBK unintegrated gluon densities," arXiv:1011.5161 [hep-ph].

[56] A. Dumitru, D. E. Kharzeev, E. M. Levin, and Y. Nara, "Gluon Saturation in *pA* Collisions at the LHC: KLN Model Predictions For Hadron Multiplicities," *Phys. Rev.* **C85** (2012) 044920, arXiv:1111.3031 [hep-ph].

[57] D. Kharzeev and E. Levin, "Manifestations of high density QCD in the first RHIC data," *Phys. Lett.* **B523** (2001) 79–87, arXiv:nucl-th/0108006 [nucl-th].

[58] D. Kharzeev, E. Levin, and M. Nardi, "Color glass condensate at the LHC: Hadron multiplicities in pp, pA and AA collisions," *Nucl. Phys.* **A747** (2005) 609–629, arXiv:hep-ph/0408050 [hep-ph].

[59] D. Kharzeev and M. Nardi, "Hadron production in nuclear collisions at RHIC and high density QCD," *Phys. Lett.* **B507** (2001) 121–128, arXiv:nucl-th/0012025 [nucl-th].

[60] N. Armesto, C. A. Salgado, and U. A. Wiedemann, "Relating high-energy lepton-hadron, proton-nucleus and nucleus-nucleus collisions through geometric scaling," *Phys. Rev. Lett.* **94** (2005) 022002, arXiv:hep-ph/0407018 [hep-ph].

[61] B. Schenke, P. Tribedy, and R. Venugopalan, "Multiplicity distributions in p+p, p+A and A+A collisions from Yang-Mills dynamics," *Phys. Rev.* **C89** no. 2, (2014) 024901, `arXiv:1311.3636 [hep-ph]`.

[62] B. Schenke, P. Tribedy, and R. Venugopalan, "Fluctuating Glasma initial conditions and flow in heavy ion collisions," *Phys. Rev. Lett.* **108** (2012) 252301, `arXiv:1202.6646 [nucl-th]`.

[63] H. Niemi, K. J. Eskola, and R. Paatelainen, "Event-by-event fluctuations in a perturbative QCD + saturation + hydrodynamics model: Determining QCD matter shear viscosity in ultrarelativistic heavy-ion collisions," *Phys. Rev.* **C93** no. 2, (2016) 024907, `arXiv:1505.02677 [hep-ph]`.

[64] H. Niemi, K. J. Eskola, R. Paatelainen, and K. Tuominen, "Predictions for 5.023 TeV Pb + Pb collisions at the CERN Large Hadron Collider," *Phys. Rev.* **C93** no. 1, (2016) 014912, `arXiv:1511.04296 [hep-ph]`.

[65] K. J. Eskola, H. Niemi, R. Paatelainen, and K. Tuominen, "Predictions for multiplicities and flow harmonics in 5.44 TeV Xe+Xe collisions at the CERN Large Hadron Collider," *Phys. Rev.* **C97** no. 3, (2018) 034911, `arXiv:1711.09803 [hep-ph]`.

[66] S. A. Bass, J. E. Bernhard, and J. S. Moreland, "Determination of Quark-Gluon-Plasma Parameters from a Global Bayesian Analysis," *Nucl. Phys.* **A967** (2017) 67–73, `arXiv:1704.07671 [nucl-th]`.

[67] J. S. Moreland, J. E. Bernhard, and S. A. Bass, "Alternative ansatz to wounded nucleon and binary collision scaling in high-energy nuclear collisions," *Phys. Rev.* **C92** no. 1, (2015) 011901, `arXiv:1412.4708 [nucl-th]`.

[68] C. Shen, Z. Qiu, H. Song, J. Bernhard, S. Bass, and U. Heinz, "The iEBE-VISHNU code package for relativistic heavy-ion collisions," *Comput. Phys. Commun.* **199** (2016) 61–85, `arXiv:1409.8164 [nucl-th]`.

[69] **PHOBOS** Collaboration, B. B. Back *et al.*, "Collision geometry scaling of Au+Au pseudorapidity density from s(NN)**(1/2) = 19.6-GeV to 200-GeV," *Phys. Rev.* **C70** (2004) 021902, `arXiv:nucl-ex/0405027 [nucl-ex]`.

[70] **ALICE** Collaboration, K. Aamodt *et al.*, "Charged–particle multiplicity density at mid–rapidity in central Pb–Pb collisions at $\sqrt{s_{NN}}$ = 2.76 TeV," *Phys. Rev. Lett.* **105** (2010) 252301, `arXiv:1011.3916 [nucl-ex]`.

[71] A. H. Rezaeian, M. Siddikov, M. Van de Klundert, and R. Venugopalan, "Analysis of combined HERA data in the Impact-Parameter dependent Saturation model," *Phys. Rev.* **D87** no. 3, (2013) 034002, `arXiv:1212.2974 [hep-ph]`.

[72] **PHOBOS** Collaboration, B. Alver *et al.*, "System size, energy and centrality dependence of pseudorapidity distributions of charged particles in relativistic heavy ion collisions," *Phys. Rev. Lett.* **102** (2009) 142301, `arXiv:0709.4008 [nucl-ex]`.

A The ALICE Collaboration

S. Acharya[138] , F.T.-. Acosta[22] , D. Adamová[94] , J. Adolfsson[81] , M.M. Aggarwal[98] , G. Aglieri Rinella[36] , M. Agnello[33] , N. Agrawal[49] , Z. Ahammed[138] , S.U. Ahn[77] , S. Aiola[143] , A. Akindinov[65] , M. Al-Turany[104] , S.N. Alam[138] , D.S.D. Albuquerque[120] , D. Aleksandrov[88] , B. Alessandro[59] , R. Alfaro Molina[73] , Y. Ali[16] , A. Alici[11 ,54 ,29] , A. Alkin[3] , J. Alme[24] , T. Alt[70] , L. Altenkamper[24] , I. Altsybeev[137] , C. Andrei[48] , D. Andreou[36] , H.A. Andrews[108] , A. Andronic[141 ,104] , M. Angeletti[36] , V. Anguelov[102] , C. Anson[17] , T. Antičić[105] , F. Antinori[57] , P. Antonioli[54] , R. Anwar[124] , N. Apadula[80] , L. Aphecetche[112] , H. Appelshäuser[70] , S. Arcelli[29] , R. Arnaldi[59] , O.W. Arnold[103 ,115] , I.C. Arsene[23] , M. Arslandok[102] , B. Audurier[112] , A. Augustinus[36] , R. Averbeck[104] , M.D. Azmi[18] , A. Badalà[56] , Y.W. Baek[61 ,42] , S. Bagnasco[59] , R. Bailhache[70] , R. Bala[99] , A. Baldisseri[134] , M. Ball[44] , R.C. Baral[86] , A.M. Barbano[28] , R. Barbera[30] , F. Barile[53] , L. Barioglio[28] , G.G. Barnaföldi[142] , L.S. Barnby[93] , V. Barret[131] , P. Bartalini[7] , K. Barth[36] , E. Bartsch[70] , N. Bastid[131] , S. Basu[140] , G. Batigne[112] , B. Batyunya[76] , P.C. Batzing[23] , J.L. Bazo Alba[109] , I.G. Bearden[89] , H. Beck[102] , C. Bedda[64] , N.K. Behera[61] , I. Belikov[133] , F. Bellini[36] , H. Bello Martinez[2] , R. Bellwied[124] , L.G.E. Beltran[118] , V. Belyaev[92] , G. Bencedi[142] , S. Beole[28] , A. Bercuci[48] , Y. Berdnikov[96] , D. Berenyi[142] , R.A. Bertens[127] , D. Berzano[36 ,59] , L. Betev[36] , P.P. Bhaduri[138] , A. Bhasin[99] , I.R. Bhat[99] , H. Bhatt[49] , B. Bhattacharjee[43] , J. Bhom[116] , A. Bianchi[28] , L. Bianchi[124] , N. Bianchi[52] , J. Bielčík[39] , J. Bielčíková[94] , A. Bilandzic[115 ,103] , G. Biro[142] , R. Biswas[4] , S. Biswas[4] , J.T. Blair[117] , D. Blau[88] , C. Blume[70] , G. Boca[135] , F. Bock[36] , A. Bogdanov[92] , L. Boldizsár[142] , M. Bombara[40] , G. Bonomi[136] , M. Bonora[36] , H. Borel[134] , A. Borissov[20 ,141] , M. Borri[126] , E. Botta[28] , C. Bourjau[89] , L. Bratrud[70] , P. Braun-Munzinger[104] , M. Bregant[119] , T.A. Broker[70] , M. Broz[39] , E.J. Brucken[45] , E. Bruna[59] , G.E. Bruno[36 ,35] , D. Budnikov[106] , H. Buesching[70] , S. Bufalino[33] , P. Buhler[111] , P. Buncic[36] , O. Busch[130 ,i] , Z. Buthelezi[74] , J.B. Butt[16] , J.T. Buxton[19] , J. Cabala[114] , D. Caffarri[90] , H. Caines[143] , A. Caliva[104] , E. Calvo Villar[109] , R.S. Camacho[2] , P. Camerini[27] , A.A. Capon[111] , F. Carena[36] , W. Carena[36] , F. Carnesecchi[29 ,11] , J. Castillo Castellanos[134] , A.J. Castro[127] , E.A.R. Casula[55] , C. Ceballos Sanchez[9] , S. Chandra[138] , B. Chang[125] , W. Chang[7] , S. Chapeland[36] , M. Chartier[126] , S. Chattopadhyay[138] , S. Chattopadhyay[107] , A. Chauvin[103 ,115] , C. Cheshkov[132] , B. Cheynis[132] , V. Chibante Barroso[36] , D.D. Chinellato[120] , S. Cho[61] , P. Chochula[36] , T. Chowdhury[131] , P. Christakoglou[90] , C.H. Christensen[89] , P. Christiansen[81] , T. Chujo[130] , S.U. Chung[20] , C. Cicalo[55] , L. Cifarelli[11 ,29] , F. Cindolo[54] , J. Cleymans[123] , F. Colamaria[53] , D. Colella[66 ,36 ,53] , A. Collu[80] , M. Colocci[29] , M. Concas[59 ,ii] , G. Conesa Balbastre[79] , Z. Conesa del Valle[62] , J.G. Contreras[39] , T.M. Cormier[95] , Y. Corrales Morales[59] , P. Cortese[34] , M.R. Cosentino[121] , F. Costa[36] , S. Costanza[135] , J. Crkovská[62] , P. Crochet[131] , E. Cuautle[71] , L. Cunqueiro[141 ,95] , T. Dahms[103 ,115] , A. Dainese[57] , S. Dani[67] , M.C. Danisch[102] , A. Danu[69] , D. Das[107] , I. Das[107] , S. Das[4] , A. Dash[86] , S. Dash[49] , S. De[50] , A. De Caro[32] , G. de Cataldo[53] , C. de Conti[119] , J. de Cuveland[41] , A. De Falco[26] , D. De Gruttola[11 ,32] , N. De Marco[59] , S. De Pasquale[32] , R.D. De Souza[120] , H.F. Degenhardt[119] , A. Deisting[104 ,102] , A. Deloff[85] , S. Delsanto[28] , C. Deplano[90] , P. Dhankher[49] , D. Di Bari[35] , A. Di Mauro[36] , B. Di Ruzza[57] , R.A. Diaz[9] , T. Dietel[123] , P. Dillenseger[70] , Y. Ding[7] , R. Divià[36] , Ø. Djuvsland[24] , A. Dobrin[36] , D. Domenicis Gimenez[119] , B. Dönigus[70] , O. Dordic[23] , L.V.R. Doremalen[64] , A.K. Dubey[138] , A. Dubla[104] , L. Ducroux[132] , S. Dudi[98] , A.K. Duggal[98] , M. Dukhishyam[86] , P. Dupieux[131] , R.J. Ehlers[143] , D. Elia[53] , E. Endress[109] , H. Engel[75] , E. Epple[143] , B. Erazmus[112] , F. Erhardt[97] , M.R. Ersdal[24] , B. Espagnon[62] , G. Eulisse[36] , J. Eum[20] , D. Evans[108] , S. Evdokimov[91] , L. Fabbietti[103 ,115] , M. Faggin[31] , J. Faivre[79] , A. Fantoni[52] , M. Fasel[95] , L. Feldkamp[141] , A. Feliciello[59] , G. Feofilov[137] , A. Fernández Téllez[2] , A. Ferretti[28] , A. Festanti[31 ,36] , V.J.G. Feuillard[102] , J. Figiel[116] , M.A.S. Figueredo[119] , S. Filchagin[106] , D. Finogeev[63] , F.M. Fionda[24] , G. Fiorenza[53] , F. Flor[124] , M. Floris[36] , S. Foertsch[74] , P. Foka[104] , S. Fokin[88] , E. Fragiacomo[60] , A. Francescon[36] , A. Francisco[112] , U. Frankenfeld[104] , G.G. Fronze[28] , U. Fuchs[36] , C. Furget[79] , A. Furs[63] , M. Fusco Girard[32] , J.J. Gaardhøje[89] , M. Gagliardi[28] , A.M. Gago[109] , K. Gajdosova[89] , M. Gallio[28] , C.D. Galvan[118] , P. Ganoti[84] , C. Garabatos[104] , E. Garcia-Solis[12] , K. Garg[30] , C. Gargiulo[36] , P. Gasik[115 ,103] , E.F. Gauger[117] , M.B. Gay Ducati[72] , M. Germain[112] , J. Ghosh[107] , P. Ghosh[138] , S.K. Ghosh[4] , P. Gianotti[52] , P. Giubellino[104 ,59] , P. Giubilato[31] , P. Glässel[102] , D.M. Gómez Coral[73] , A. Gomez Ramirez[75] , V. Gonzalez[104] , P. González-Zamora[2] , S. Gorbunov[41] , L. Görlich[116] , S. Gotovac[37] , V. Grabski[73] , L.K. Graczykowski[139] , K.L. Graham[108] , L. Greiner[80] , A. Grelli[64] , C. Grigoras[36] , V. Grigoriev[92] , A. Grigoryan[1] , S. Grigoryan[76] , J.M. Gronefeld[104] , F. Grosa[33] , J.F. Grosse-Oetringhaus[36] , R. Grosso[104] , R. Guernane[79] , B. Guerzoni[29] , M. Guittiere[112] , K. Gulbrandsen[89] , T. Gunji[129] , A. Gupta[99] , R. Gupta[99] , I.B. Guzman[2] , R. Haake[36] , M.K. Habib[104] , C. Hadjidakis[62] , H. Hamagaki[82] , G. Hamar[142] , M. Hamid[7] , J.C. Hamon[133] , R. Hannigan[117] , M.R. Haque[64] , J.W. Harris[143] , A. Harton[12] , H. Hassan[79] , D. Hatzifotiadou[54 ,11] , S. Hayashi[129] , S.T. Heckel[70] , E. Hellbär[70] , H. Helstrup[38] , A. Herghelegiu[48] , E.G. Hernandez[2] , G. Herrera Corral[10] , F. Herrmann[141] , K.F. Hetland[38] , T.E. Hilden[45] , H. Hillemanns[36] , C. Hills[126] , B. Hippolyte[133] , B. Hohlweger[103] , D. Horak[39] , S. Hornung[104] , R. Hosokawa[130 ,79] , J. Hota[67] , P. Hristov[36] , C. Huang[62] , C. Hughes[127] , P. Huhn[70] ,

T.J. Humanic[19], H. Hushnud[107], N. Hussain[43], T. Hussain[18], D. Hutter[41], D.S. Hwang[21], J.P. Iddon[126], S.A. Iga Buitron[71], R. Ilkaev[106], M. Inaba[130], M. Ippolitov[88], M.S. Islam[107], M. Ivanov[104], V. Ivanov[96], V. Izucheev[91], B. Jacak[80], N. Jacazio[29], P.M. Jacobs[80], M.B. Jadhav[49], S. Jadlovska[114], J. Jadlovsky[114], S. Jaelani[64], C. Jahnke[119 ,115], M.J. Jakubowska[139], M.A. Janik[139], C. Jena[86], M. Jercic[97], R.T. Jimenez Bustamante[104], M. Jin[124], P.G. Jones[108], A. Jusko[108], P. Kalinak[66], A. Kalweit[36], J.H. Kang[144], V. Kaplin[92], S. Kar[7], A. Karasu Uysal[78], O. Karavichev[63], T. Karavicheva[63], P. Karczmarczyk[36], E. Karpechev[63], U. Kebschull[75], R. Keidel[47], D.L.D. Keijdener[64], M. Keil[36], B. Ketzer[44], Z. Khabanova[90], A.M. Khan[7], S. Khan[18], S.A. Khan[138], A. Khanzadeev[96], Y. Kharlov[91], A. Khatun[18], A. Khuntia[50], M.M. Kielbowicz[116], B. Kileng[38], B. Kim[61], B. Kim[130], D. Kim[144], D.J. Kim[125], E.J. Kim[14], H. Kim[144], J.S. Kim[42], J. Kim[102], M. Kim[61 ,102], S. Kim[21], T. Kim[144], T. Kim[144], S. Kirsch[41], I. Kisel[41], S. Kiselev[65], A. Kisiel[139], J.L. Klay[6], C. Klein[70], J. Klein[36 ,59], C. Klein-Bösing[141], S. Klewin[102], A. Kluge[36], M.L. Knichel[36], A.G. Knospe[124], C. Kobdaj[113], M. Kofarago[142], M.K. Köhler[102], T. Kollegger[104], N. Kondratyeva[92], E. Kondratyuk[91], A. Konevskikh[63], M. Konyushikhin[140], O. Kovalenko[85], V. Kovalenko[137], M. Kowalski[116], I. Králik[66], A. Kravčáková[40], L. Kreis[104], M. Krivda[66 ,108], F. Krizek[94], M. Krüger[70], E. Kryshen[96], M. Krzewicki[41], A.M. Kubera[19], V. Kučera[94 ,61], C. Kuhn[133], P.G. Kuijer[90], J. Kumar[49], L. Kumar[98], S. Kumar[49], S. Kundu[86], P. Kurashvili[85], A. Kurepin[63], A.B. Kurepin[63], A. Kuryakin[106], S. Kushpil[94], M.J. Kweon[61], Y. Kwon[144], S.L. La Pointe[41], P. La Rocca[30], Y.S. Lai[80], I. Lakomov[36], R. Langoy[122], K. Lapidus[143], C. Lara[75], A. Lardeux[23], P. Larionov[52], E. Laudi[36], R. Lavicka[39], R. Lea[27], L. Leardini[102], S. Lee[144], F. Lehas[90], S. Lehner[111], J. Lehrbach[41], R.C. Lemmon[93], I. León Monzón[118], P. Lévai[142], X. Li[13], X.L. Li[7], J. Lien[122], R. Lietava[108], B. Lim[20], S. Lindal[23], V. Lindenstruth[41], S.W. Lindsay[126], C. Lippmann[104], M.A. Lisa[19], V. Litichevskyi[45], A. Liu[80], H.M. Ljunggren[81], W.J. Llope[140], D.F. Lodato[64], V. Loginov[92], C. Loizides[95 ,80], P. Loncar[37], X. Lopez[131], E. López Torres[9], A. Lowe[142], P. Luettig[70], J.R. Luhder[141], M. Lunardon[31], G. Luparello[60], M. Lupi[36], A. Maevskaya[63], M. Mager[36], S.M. Mahmood[23], A. Maire[133], R.D. Majka[143], M. Malaev[96], Q.W. Malik[23], L. Malinina[76 ,iii], D. Mal'Kevich[65], P. Malzacher[104], A. Mamonov[106], V. Manko[88], F. Manso[131], V. Manzari[53], Y. Mao[7], M. Marchisone[74 ,128 ,132], J. Mareš[68], G.V. Margagliotti[27], A. Margotti[54], J. Margutti[64], A. Marín[104], C. Markert[117], M. Marquard[70], N.A. Martin[104], P. Martinengo[36], J.L. Martinez[124], M.I. Martínez[2], G. Martínez García[112], M. Martinez Pedreira[36], S. Masciocchi[104], M. Masera[28], A. Masoni[55], L. Massacrier[62], E. Masson[112], A. Mastroserio[53], A.M. Mathis[103 ,115], P.F.T. Matuoka[119], A. Matyja[127 ,116], C. Mayer[116], M. Mazzilli[35], M.A. Mazzoni[58], F. Meddi[25], Y. Melikyan[92], A. Menchaca-Rocha[73], E. Meninno[32], J. Mercado Pérez[102], M. Meres[15], C.S. Meza[109], S. Mhlanga[123], Y. Miake[130], L. Micheletti[28], M.M. Mieskolainen[45], D.L. Mihaylov[103], K. Mikhaylov[65 ,76], A. Mischke[64], A.N. Mishra[71], D. Miśkowiec[104], J. Mitra[138], C.M. Mitu[69], N. Mohammadi[36], A.P. Mohanty[64], B. Mohanty[86], M. Mohisin Khan[18 ,iv], D.A. Moreira De Godoy[141], L.A.P. Moreno[2], S. Moretto[31], A. Morreale[112], A. Morsch[36], V. Muccifora[52], E. Mudnic[37], D. Mühlheim[141], S. Muhuri[138], M. Mukherjee[4], J.D. Mulligan[143], M.G. Munhoz[119], K. Münning[44], M.I.A. Munoz[80], R.H. Munzer[70], H. Murakami[129], S. Murray[74], L. Musa[36], J. Musinsky[66], C.J. Myers[124], J.W. Myrcha[139], B. Naik[49], R. Nair[85], B.K. Nandi[49], R. Nania[54 ,11], E. Nappi[53], A. Narayan[49], M.U. Naru[16], A.F. Nassirpour[81], H. Natal da Luz[119], C. Nattrass[127], S.R. Navarro[2], K. Nayak[86], R. Nayak[49], T.K. Nayak[138], S. Nazarenko[106], R.A. Negrao De Oliveira[70 ,36], L. Nellen[71], S.V. Nesbo[38], G. Neskovic[41], F. Ng[124], M. Nicassio[104], J. Niedziela[139 ,36], B.S. Nielsen[89], S. Nikolaev[88], S. Nikulin[88], V. Nikulin[96], F. Noferini[11 ,54], P. Nomokonov[76], G. Nooren[64], J.C.C. Noris[2], J. Norman[79], A. Nyanin[88], J. Nystrand[24], H. Oh[144], A. Ohlson[102], J. Oleniacz[139], A.C. Oliveira Da Silva[119], M.H. Oliver[143], J. Onderwaater[104], C. Oppedisano[59], R. Orava[45], M. Oravec[114], A. Ortiz Velasquez[71], A. Oskarsson[81], J. Otwinowski[116], K. Oyama[82], Y. Pachmayer[102], V. Pacik[89], D. Pagano[136], G. Paić[71], P. Palni[7], J. Pan[140], A.K. Pandey[49], S. Panebianco[134], V. Papikyan[1], P. Pareek[50], J. Park[61], J.E. Parkkila[125], S. Parmar[98], A. Passfeld[141], S.P. Pathak[124], R.N. Patra[138], B. Paul[59], H. Pei[7], T. Peitzmann[64], X. Peng[7], L.G. Pereira[72], H. Pereira Da Costa[134], D. Peresunko[88], E. Perez Lezama[70], V. Peskov[70], Y. Pestov[5], V. Petráček[39], M. Petrovici[48], C. Petta[30], R.P. Pezzi[72], S. Piano[60], M. Pikna[15], P. Pillot[112], L.O.D.L. Pimentel[89], O. Pinazza[54 ,36], L. Pinsky[124], S. Pisano[52], D.B. Piyarathna[124], M. Płoskoń[80], M. Planinic[97], F. Pliquett[70], J. Pluta[139], S. Pochybova[142], P.L.M. Podesta-Lerma[118], M.G. Poghosyan[95], B. Polichtchouk[91], N. Poljak[97], W. Poonsawat[113], A. Pop[48], H. Poppenborg[141], S. Porteboeuf-Houssais[131], V. Pozdniakov[76], S.K. Prasad[4], R. Preghenella[54], F. Prino[59], C.A. Pruneau[140], I. Pshenichnov[63], M. Puccio[28], V. Punin[106], J. Putschke[140], S. Raha[4], S. Rajput[99], J. Rak[125], A. Rakotozafindrabe[134], L. Ramello[34], F. Rami[133], R. Raniwala[100], S. Raniwala[100], S.S. Räsänen[45], B.T. Rascanu[70], V. Ratza[44], I. Ravasenga[33], K.F. Read[127 ,95], K. Redlich[85 ,v], A. Rehman[24], P. Reichelt[70], F. Reidt[36], X. Ren[7], R. Renfordt[70], A. Reshetin[63], J.-P. Revol[11], K. Reygers[102], V. Riabov[96], T. Richert[64 ,81], M. Richter[23], P. Riedler[36], W. Riegler[36], F. Riggi[30], C. Ristea[69], S.P. Rode[50], M. Rodríguez Cahuantzi[2], K. Røed[23], R. Rogalev[91], E. Rogochaya[76], D. Rohr[36], D. Röhrich[24], P.S. Rokita[139],

F. Ronchetti[52] , E.D. Rosas[71] , K. Roslon[139] , P. Rosnet[131] , A. Rossi[31] , A. Rotondi[135] , F. Roukoutakis[84] ,
C. Roy[133] , P. Roy[107] , O.V. Rueda[71] , R. Rui[27] , B. Rumyantsev[76] , A. Rustamov[87] , E. Ryabinkin[88] ,
Y. Ryabov[96] , A. Rybicki[116] , S. Saarinen[45] , S. Sadhu[138] , S. Sadovsky[91] , K. Šafařík[36] , S.K. Saha[138] ,
B. Sahoo[49] , P. Sahoo[50] , R. Sahoo[50] , S. Sahoo[67] , P.K. Sahu[67] , J. Saini[138] , S. Sakai[130] , M.A. Saleh[140] ,
S. Sambyal[99] , V. Samsonov[96 ,92] , A. Sandoval[73] , A. Sarkar[74] , D. Sarkar[138] , N. Sarkar[138] , P. Sarma[43] ,
M.H.P. Sas[64] , E. Scapparone[54] , F. Scarlassara[31] , B. Schaefer[95] , H.S. Scheid[70] , C. Schiaua[48] , R. Schicker[102] ,
C. Schmidt[104] , H.R. Schmidt[101] , M.O. Schmidt[102] , M. Schmidt[101] , N.V. Schmidt[95 ,70] , J. Schukraft[36] ,
Y. Schutz[36 ,133] , K. Schwarz[104] , K. Schweda[104] , G. Scioli[29] , E. Scomparin[59] , M. Šefčík[40] , J.E. Seger[17] ,
Y. Sekiguchi[129] , D. Sekihata[46] , I. Selyuzhenkov[104 ,92] , K. Senosi[74] , S. Senyukov[133] , E. Serradilla[73] , P. Sett[49] ,
A. Sevcenco[69] , A. Shabanov[63] , A. Shabetai[112] , R. Shahoyan[36] , W. Shaikh[107] , A. Shangaraev[91] , A. Sharma[98] ,
A. Sharma[99] , M. Sharma[99] , N. Sharma[98] , A.I. Sheikh[138] , K. Shigaki[46] , M. Shimomura[83] , S. Shirinkin[65] ,
Q. Shou[7 ,110] , K. Shtejer[28] , Y. Sibiriak[88] , S. Siddhanta[55] , K.M. Sielewicz[36] , T. Siemiarczuk[85] , D. Silvermyr[81] ,
G. Simatovic[90] , G. Simonetti[36 ,103] , R. Singaraju[138] , R. Singh[86] , R. Singh[99] , V. Singhal[138] , T. Sinha[107] ,
B. Sitar[15] , M. Sitta[34] , T.B. Skaali[23] , M. Slupecki[125] , N. Smirnov[143] , R.J.M. Snellings[64] , T.W. Snellman[125] ,
J. Song[20] , F. Soramel[31] , S. Sorensen[127] , F. Sozzi[104] , I. Sputowska[116] , J. Stachel[102] , I. Stan[69] , P. Stankus[95] ,
E. Stenlund[81] , D. Stocco[112] , M.M. Storetvedt[38] , P. Strmen[15] , A.A.P. Suaide[119] , T. Sugitate[46] , C. Suire[62] ,
M. Suleymanov[16] , M. Suljic[36 ,27] , R. Sultanov[65] , M. Šumbera[94] , S. Sumowidagdo[51] , K. Suzuki[111] ,
S. Swain[67] , A. Szabo[15] , I. Szarka[15] , U. Tabassam[16] , J. Takahashi[120] , G.J. Tambave[24] , N. Tanaka[130] ,
M. Tarhini[112] , M. Tariq[18] , M.G. Tarzila[48] , A. Tauro[36] , G. Tejeda Muñoz[2] , A. Telesca[36] , C. Terrevoli[31] ,
B. Teyssier[132] , D. Thakur[50] , S. Thakur[138] , D. Thomas[117] , F. Thoresen[89] , R. Tieulent[132] , A. Tikhonov[63] ,
A.R. Timmins[124] , A. Toia[70] , N. Topilskaya[63] , M. Toppi[52] , S.R. Torres[118] , S. Tripathy[50] , S. Trogolo[28] ,
G. Trombetta[35] , L. Tropp[40] , V. Trubnikov[3] , W.H. Trzaska[125] , T.P. Trzcinski[139] , B.A. Trzeciak[64] , T. Tsuji[129] ,
A. Tumkin[106] , R. Turrisi[57] , T.S. Tveter[23] , K. Ullaland[24] , E.N. Umaka[124] , A. Uras[132] , G.L. Usai[26] ,
A. Utrobicic[97] , M. Vala[114] , J.W. Van Hoorne[36] , M. van Leeuwen[64] , P. Vande Vyvre[36] , D. Varga[142] ,
A. Vargas[2] , M. Vargyas[125] , R. Varma[49] , M. Vasileiou[84] , A. Vasiliev[88] , A. Vauthier[79] , O. Vázquez Doce[103 ,115] ,
V. Vechernin[137] , A.M. Veen[64] , E. Vercellin[28] , S. Vergara Limón[2] , L. Vermunt[64] , R. Vernet[8] , R. Vértesi[142] ,
L. Vickovic[37] , J. Viinikainen[125] , Z. Vilakazi[128] , O. Villalobos Baillie[108] , A. Villatoro Tello[2] , A. Vinogradov[88] ,
T. Virgili[32] , V. Vislavicius[89 ,81] , A. Vodopyanov[76] , M.A. Völkl[101] , K. Voloshin[65] , S.A. Voloshin[140] ,
G. Volpe[35] , B. von Haller[36] , I. Vorobyev[115 ,103] , D. Voscek[114] , D. Vranic[104 ,36] , J. Vrláková[40] , B. Wagner[24] ,
H. Wang[64] , M. Wang[7] , Y. Watanabe[130] , M. Weber[111] , S.G. Weber[104] , A. Wegrzynek[36] , D.F. Weiser[102] ,
S.C. Wenzel[36] , J.P. Wessels[141] , U. Westerhoff[141] , A.M. Whitehead[123] , J. Wiechula[70] , J. Wikne[23] , G. Wilk[85] ,
J. Wilkinson[54] , G.A. Willems[141 ,36] , M.C.S. Williams[54] , E. Willsher[108] , B. Windelband[102] , W.E. Witt[127] ,
R. Xu[7] , S. Yalcin[78] , K. Yamakawa[46] , S. Yano[46] , Z. Yin[7] , H. Yokoyama[79 ,130] , I.-K. Yoo[20] , J.H. Yoon[61] ,
V. Yurchenko[3] , V. Zaccolo[59] , A. Zaman[16] , C. Zampolli[36] , H.J.C. Zanoli[119] , N. Zardoshti[108] ,
A. Zarochentsev[137] , P. Závada[68] , N. Zaviyalov[106] , H. Zbroszczyk[139] , M. Zhalov[96] , X. Zhang[7] , Y. Zhang[7] ,
Z. Zhang[7 ,131] , C. Zhao[23] , V. Zherebchevskii[137] , N. Zhigareva[65] , D. Zhou[7] , Y. Zhou[89] , Z. Zhou[24] , H. Zhu[7] ,
J. Zhu[7] , Y. Zhu[7] , A. Zichichi[29 ,11] , M.B. Zimmermann[36] , G. Zinovjev[3] , J. Zmeskal[111] , S. Zou[7] ,

Affiliation notes

[i] Deceased
[ii] Dipartimento DET del Politecnico di Torino, Turin, Italy
[iii] M.V. Lomonosov Moscow State University, D.V. Skobeltsyn Institute of Nuclear, Physics, Moscow, Russia
[iv] Department of Applied Physics, Aligarh Muslim University, Aligarh, India
[v] Institute of Theoretical Physics, University of Wroclaw, Poland

Collaboration Institutes

[1] A.I. Alikhanyan National Science Laboratory (Yerevan Physics Institute) Foundation, Yerevan, Armenia
[2] Benemérita Universidad Autónoma de Puebla, Puebla, Mexico
[3] Bogolyubov Institute for Theoretical Physics, National Academy of Sciences of Ukraine, Kiev, Ukraine
[4] Bose Institute, Department of Physics and Centre for Astroparticle Physics and Space Science (CAPSS), Kolkata, India
[5] Budker Institute for Nuclear Physics, Novosibirsk, Russia
[6] California Polytechnic State University, San Luis Obispo, California, United States
[7] Central China Normal University, Wuhan, China
[8] Centre de Calcul de l'IN2P3, Villeurbanne, Lyon, France

[9]   Centro de Aplicaciones Tecnológicas y Desarrollo Nuclear (CEADEN), Havana, Cuba

[10] Centro de Investigación y de Estudios Avanzados (CINVESTAV), Mexico City and Mérida, Mexico

[11] Centro Fermi - Museo Storico della Fisica e Centro Studi e Ricerche "Enrico Fermi', Rome, Italy

[12] Chicago State University, Chicago, Illinois, United States

[13] China Institute of Atomic Energy, Beijing, China

[14] Chonbuk National University, Jeonju, Republic of Korea

[15] Comenius University Bratislava, Faculty of Mathematics, Physics and Informatics, Bratislava, Slovakia

[16] COMSATS Institute of Information Technology (CIIT), Islamabad, Pakistan

[17] Creighton University, Omaha, Nebraska, United States

[18] Department of Physics, Aligarh Muslim University, Aligarh, India

[19] Department of Physics, Ohio State University, Columbus, Ohio, United States

[20] Department of Physics, Pusan National University, Pusan, Republic of Korea

[21] Department of Physics, Sejong University, Seoul, Republic of Korea

[22] Department of Physics, University of California, Berkeley, California, United States

[23] Department of Physics, University of Oslo, Oslo, Norway

[24] Department of Physics and Technology, University of Bergen, Bergen, Norway

[25] Dipartimento di Fisica dell'Università 'La Sapienza' and Sezione INFN, Rome, Italy

[26] Dipartimento di Fisica dell'Università and Sezione INFN, Cagliari, Italy

[27] Dipartimento di Fisica dell'Università and Sezione INFN, Trieste, Italy

[28] Dipartimento di Fisica dell'Università and Sezione INFN, Turin, Italy

[29] Dipartimento di Fisica e Astronomia dell'Università and Sezione INFN, Bologna, Italy

[30] Dipartimento di Fisica e Astronomia dell'Università and Sezione INFN, Catania, Italy

[31] Dipartimento di Fisica e Astronomia dell'Università and Sezione INFN, Padova, Italy

[32] Dipartimento di Fisica 'E.R. Caianiello' dell'Università and Gruppo Collegato INFN, Salerno, Italy

[33] Dipartimento DISAT del Politecnico and Sezione INFN, Turin, Italy

[34] Dipartimento di Scienze e Innovazione Tecnologica dell'Università del Piemonte Orientale and INFN Sezione di Torino, Alessandria, Italy

[35] Dipartimento Interateneo di Fisica 'M. Merlin' and Sezione INFN, Bari, Italy

[36] European Organization for Nuclear Research (CERN), Geneva, Switzerland

[37] Faculty of Electrical Engineering, Mechanical Engineering and Naval Architecture, University of Split, Split, Croatia

[38] Faculty of Engineering and Science, Western Norway University of Applied Sciences, Bergen, Norway

[39] Faculty of Nuclear Sciences and Physical Engineering, Czech Technical University in Prague, Prague, Czech Republic

[40] Faculty of Science, P.J. Šafárik University, Košice, Slovakia

[41] Frankfurt Institute for Advanced Studies, Johann Wolfgang Goethe-Universität Frankfurt, Frankfurt, Germany

[42] Gangneung-Wonju National University, Gangneung, Republic of Korea

[43] Gauhati University, Department of Physics, Guwahati, India

[44] Helmholtz-Institut für Strahlen- und Kernphysik, Rheinische Friedrich-Wilhelms-Universität Bonn, Bonn, Germany

[45] Helsinki Institute of Physics (HIP), Helsinki, Finland

[46] Hiroshima University, Hiroshima, Japan

[47] Hochschule Worms, Zentrum für Technologietransfer und Telekommunikation (ZTT), Worms, Germany

[48] Horia Hulubei National Institute of Physics and Nuclear Engineering, Bucharest, Romania

[49] Indian Institute of Technology Bombay (IIT), Mumbai, India

[50] Indian Institute of Technology Indore, Indore, India

[51] Indonesian Institute of Sciences, Jakarta, Indonesia

[52] INFN, Laboratori Nazionali di Frascati, Frascati, Italy

[53] INFN, Sezione di Bari, Bari, Italy

[54] INFN, Sezione di Bologna, Bologna, Italy

[55] INFN, Sezione di Cagliari, Cagliari, Italy

[56] INFN, Sezione di Catania, Catania, Italy

[57] INFN, Sezione di Padova, Padova, Italy

[58] INFN, Sezione di Roma, Rome, Italy

[59] INFN, Sezione di Torino, Turin, Italy

23

[60] INFN, Sezione di Trieste, Trieste, Italy

[61] Inha University, Incheon, Republic of Korea

[62] Institut de Physique Nucléaire d'Orsay (IPNO), Institut National de Physique Nucléaire et de Physique des Particules (IN2P3/CNRS), Université de Paris-Sud, Université Paris-Saclay, Orsay, France

[63] Institute for Nuclear Research, Academy of Sciences, Moscow, Russia

[64] Institute for Subatomic Physics, Utrecht University/Nikhef, Utrecht, Netherlands

[65] Institute for Theoretical and Experimental Physics, Moscow, Russia

[66] Institute of Experimental Physics, Slovak Academy of Sciences, Košice, Slovakia

[67] Institute of Physics, Bhubaneswar, India

[68] Institute of Physics of the Czech Academy of Sciences, Prague, Czech Republic

[69] Institute of Space Science (ISS), Bucharest, Romania

[70] Institut für Kernphysik, Johann Wolfgang Goethe-Universität Frankfurt, Frankfurt, Germany

[71] Instituto de Ciencias Nucleares, Universidad Nacional Autónoma de México, Mexico City, Mexico

[72] Instituto de Física, Universidade Federal do Rio Grande do Sul (UFRGS), Porto Alegre, Brazil

[73] Instituto de Física, Universidad Nacional Autónoma de México, Mexico City, Mexico

[74] iThemba LABS, National Research Foundation, Somerset West, South Africa

[75] Johann-Wolfgang-Goethe Universität Frankfurt Institut für Informatik, Fachbereich Informatik und Mathematik, Frankfurt, Germany

[76] Joint Institute for Nuclear Research (JINR), Dubna, Russia

[77] Korea Institute of Science and Technology Information, Daejeon, Republic of Korea

[78] KTO Karatay University, Konya, Turkey

[79] Laboratoire de Physique Subatomique et de Cosmologie, Université Grenoble-Alpes, CNRS-IN2P3, Grenoble, France

[80] Lawrence Berkeley National Laboratory, Berkeley, California, United States

[81] Lund University Department of Physics, Division of Particle Physics, Lund, Sweden

[82] Nagasaki Institute of Applied Science, Nagasaki, Japan

[83] Nara Women's University (NWU), Nara, Japan

[84] National and Kapodistrian University of Athens, School of Science, Department of Physics , Athens, Greece

[85] National Centre for Nuclear Research, Warsaw, Poland

[86] National Institute of Science Education and Research, HBNI, Jatni, India

[87] National Nuclear Research Center, Baku, Azerbaijan

[88] National Research Centre Kurchatov Institute, Moscow, Russia

[89] Niels Bohr Institute, University of Copenhagen, Copenhagen, Denmark

[90] Nikhef, National institute for subatomic physics, Amsterdam, Netherlands

[91] NRC Kurchatov Institute IHEP, Protvino, Russia

[92] NRNU Moscow Engineering Physics Institute, Moscow, Russia

[93] Nuclear Physics Group, STFC Daresbury Laboratory, Daresbury, United Kingdom

[94] Nuclear Physics Institute of the Czech Academy of Sciences, Řež u Prahy, Czech Republic

[95] Oak Ridge National Laboratory, Oak Ridge, Tennessee, United States

[96] Petersburg Nuclear Physics Institute, Gatchina, Russia

[97] Physics department, Faculty of science, University of Zagreb, Zagreb, Croatia

[98] Physics Department, Panjab University, Chandigarh, India

[99] Physics Department, University of Jammu, Jammu, India

[100] Physics Department, University of Rajasthan, Jaipur, India

[101] Physikalisches Institut, Eberhard-Karls-Universität Tübingen, Tübingen, Germany

[102] Physikalisches Institut, Ruprecht-Karls-Universität Heidelberg, Heidelberg, Germany

[103] Physik Department, Technische Universität München, Munich, Germany

[104] Research Division and ExtreMe Matter Institute EMMI, GSI Helmholtzzentrum für Schwerionenforschung GmbH, Darmstadt, Germany

[105] Rudjer Bošković Institute, Zagreb, Croatia

[106] Russian Federal Nuclear Center (VNIIEF), Sarov, Russia

[107] Saha Institute of Nuclear Physics, Kolkata, India

[108] School of Physics and Astronomy, University of Birmingham, Birmingham, United Kingdom

[109] Sección Física, Departamento de Ciencias, Pontificia Universidad Católica del Perú, Lima, Peru

[110] Shanghai Institute of Applied Physics, Shanghai, China

[111] Stefan Meyer Institut für Subatomare Physik (SMI), Vienna, Austria
[112] SUBATECH, IMT Atlantique, Université de Nantes, CNRS-IN2P3, Nantes, France
[113] Suranaree University of Technology, Nakhon Ratchasima, Thailand
[114] Technical University of Košice, Košice, Slovakia
[115] Technische Universität München, Excellence Cluster 'Universe', Munich, Germany
[116] The Henryk Niewodniczanski Institute of Nuclear Physics, Polish Academy of Sciences, Cracow, Poland
[117] The University of Texas at Austin, Austin, Texas, United States
[118] Universidad Autónoma de Sinaloa, Culiacán, Mexico
[119] Universidade de São Paulo (USP), São Paulo, Brazil
[120] Universidade Estadual de Campinas (UNICAMP), Campinas, Brazil
[121] Universidade Federal do ABC, Santo Andre, Brazil
[122] University College of Southeast Norway, Tonsberg, Norway
[123] University of Cape Town, Cape Town, South Africa
[124] University of Houston, Houston, Texas, United States
[125] University of Jyväskylä, Jyväskylä, Finland
[126] University of Liverpool, Department of Physics Oliver Lodge Laboratory , Liverpool, United Kingdom
[127] University of Tennessee, Knoxville, Tennessee, United States
[128] University of the Witwatersrand, Johannesburg, South Africa
[129] University of Tokyo, Tokyo, Japan
[130] University of Tsukuba, Tsukuba, Japan
[131] Université Clermont Auvergne, CNRS/IN2P3, LPC, Clermont-Ferrand, France
[132] Université de Lyon, Université Lyon 1, CNRS/IN2P3, IPN-Lyon, Villeurbanne, Lyon, France
[133] Université de Strasbourg, CNRS, IPHC UMR 7178, F-67000 Strasbourg, France, Strasbourg, France
[134] Université Paris-Saclay Centre dÉtudes de Saclay (CEA), IRFU, Department de Physique Nucléaire (DPhN), Saclay, France
[135] Università degli Studi di Pavia, Pavia, Italy
[136] Università di Brescia, Brescia, Italy
[137] V. Fock Institute for Physics, St. Petersburg State University, St. Petersburg, Russia
[138] Variable Energy Cyclotron Centre, Kolkata, India
[139] Warsaw University of Technology, Warsaw, Poland
[140] Wayne State University, Detroit, Michigan, United States
[141] Westfälische Wilhelms-Universität Münster, Institut für Kernphysik, Münster, Germany
[142] Wigner Research Centre for Physics, Hungarian Academy of Sciences, Budapest, Hungary
[143] Yale University, New Haven, Connecticut, United States
[144] Yonsei University, Seoul, Republic of Korea